

AD_____

Award Number: DAMD17-99-1-9548

TITLE: NF2 in Hrs-Mediated Signal Transduction

PRINCIPAL INVESTIGATOR: Stefan M. Pulst, M.D.

CONTRACTING ORGANIZATION: Cedars-Sinai Medical Center
Los Angeles, California 90048

REPORT DATE: November 2001

TYPE OF REPORT: Annual

PREPARED FOR: U.S. Army Medical Research and Materiel Command
Fort Detrick, Maryland 21702-5012

DISTRIBUTION STATEMENT: Approved for Public Release;
Distribution Unlimited

The views, opinions and/or findings contained in this report are those of the author(s) and should not be construed as an official Department of the Army position, policy or decision unless so designated by other documentation.

20020416 114

REPORT DOCUMENTATION PAGE

Form Approved
OMB No. 074-0188

Public reporting burden for this collection of information is estimated to average 1 hour per response, including the time for reviewing instructions, searching existing data sources, gathering and maintaining the data needed, and completing and reviewing this collection of information. Send comments regarding this burden estimate or any other aspect of this collection of information, including suggestions for reducing this burden to Washington Headquarters Services, Directorate for Information Operations and Reports, 1215 Jefferson Davis Highway, Suite 1204, Arlington, VA 22202-4302, and to the Office of Management and Budget, Paperwork Reduction Project (0704-0188), Washington, DC 20503

| | | | | |
|--|---|--|---|---|
| 1. AGENCY USE ONLY (Leave blank) | | 2. REPORT DATE November 2001 | 3. REPORT TYPE AND DATES COVERED Annual (1 Oct 00 - 1 Oct 01) | |
| 4. TITLE AND SUBTITLE NF2 in Hrs-Mediated Signal Transduction | | | 5. FUNDING NUMBERS DAMD17-99-1-9548 | |
| 6. AUTHOR(S) Stefan M. Pulst, M.D. | | | | |
| 7. PERFORMING ORGANIZATION NAME(S) AND ADDRESS(ES) Cedars-Sinai Medical Center Los Angeles, California 90048 E-Mail: Pulst@CSHS.org | | | 8. PERFORMING ORGANIZATION REPORT NUMBER | |
| 9. SPONSORING / MONITORING AGENCY NAME(S) AND ADDRESS(ES) U.S. Army Medical Research and Materiel Command Fort Detrick, Maryland 21702-5012 | | | 10. SPONSORING / MONITORING AGENCY REPORT NUMBER | |
| 11. SUPPLEMENTARY NOTES | | | | |
| 12a. DISTRIBUTION / AVAILABILITY STATEMENT Approved for Public Release; Distribution Unlimited | | | | 12b. DISTRIBUTION CODE |
| 13. Abstract (Maximum 200 Words) (abstract should contain no proprietary or confidential information) We have identified Hrs (<u>h</u> epatocyte growth factor- <u>r</u> egulated tyrosine kinase <u>s</u> ubstrate) as an NF2 binding protein using the yeast two-hybrid system. Hrs is also known to interact with STAM (signal transduction adaptor molecule. Hrs appears to have growth suppressing functions at least in part mediated via binding to STAM with a resulting reduction in DNA synthesis. Progress is discussed in order of the three specific aims that were proposed originally: 1) Regulated overexpression of HRS in rat schwannoma cells results in similar effects as overexpression of schwannomin. This includes growth inhibition, decreased motility and abnormalities in cell spreading (Gutmann et al. 2001). 2) A recently emerging function for Hrs is the sorting of endosomes containing EGR-receptor. We have begun to examine this effect in RT4 cells overexpressing Hrs or schwannomin. 3) We have begun to generate mouse embryonic fibroblast cell lines that express schwannomin or HRS under the control of the tet-regulatable promotor. These lines will be used to examine the effects of overexpression of either protein on proliferation and STAT signaling. | | | | |
| 14. SUBJECT TERMS | | | | 15. NUMBER OF PAGES 23 16. PRICE CODE |
| 17. SECURITY CLASSIFICATION OF REPORT Unclassified | 18. SECURITY CLASSIFICATION OF THIS PAGE Unclassified | 19. SECURITY CLASSIFICATION OF ABSTRACT Unclassified | 20. LIMITATION OF ABSTRACT Unlimited | |

NSN 7540-01-280-5500

Standard Form 298 (Rev. 2-89)
Prescribed by ANSI Std. Z39-18
298-102

Table of contents

| | |
|--|----------------------|
| Cover..... | Page 1 |
| SAF 298..... | Page 2 |
| Table of Contents..... | Page 3 |
| Introduction..... | Page 4 |
| Body..... | Page 5 |
| Key Research Accomplishments..... | Page 5 |
| Reportable Outcomes..... | Page 6 |
| Conclusions..... | Page 6 |
| References..... | N/A |
| Appendices..... | 2 Manuscripts |

INTRO

Identification of signaling pathways for NF2 action is critical not only for understanding NF2 function at the molecular level, but also for the future development of novel drug treatments. We have identified Hrs (hepatocyte growth factor-regulated tyrosine kinase substrate) as an NF2 binding protein using the yeast two-hybrid system. Hrs is also known to interact with STAM (signal transduction adaptor molecule) which in turn interacts with Jak/STAT kinases. Hrs appears to have growth suppressing functions at least in part mediated via binding to STAM with a resulting reduction in DNA synthesis. We have verified Hrs-schwannomin interaction by demonstrating that Hrs can be co-immunoprecipitated using anti-schwannomin antibodies and by showing that schwannomin can be co-immunoprecipitated using anti-Hrs antibodies. We are postulating that the presence of schwannomin is critical for the stability of Hrs. In addition, we are hypothesizing that schwannomin is important for Hrs STAM interaction, and is thus involved in Jak/STAT mediated signaling pathways.

CDMRP-sponsored Research Progress Report

The Principal Investigator, Dr. Pulst has received previous funding by the CDMRP.

Award number: DAMD 17-99-1-9548
 Title: NF2 in Hrs-mediated signal transduction.
 PI Name: Stefan-M. Pulst
 Award Period 10/1/99-9/30/2002.

Key research findings (as of 9-1-2001)

Funding was received to characterize the interaction of the NF2 protein with a protein identified by yeast to-hybrid screening. In the last year, one additional manuscript has been published in the journal Human Molecular Genetics in collaboration with Dr. D. Gutmann. This manuscript is appended. Two additional manuscripts are in preparation.

- The NF2 protein interacts with Hepatocyte Growth Factor-Regulated Tyrosine Kinase Substrate (hrs) in yeast two-hybrid interactions as well as by in vitro binding.
- NF2 protein and hrs are co-localized to early endosomes.
- Overexpression of Hrs results in changes in EGF-receptor trafficking.
- Overexpression of NF2 results in changes in EGF-receptor trafficking. These changes are substrate-dependent.
- Mouse embryonic fibroblasts can be engineered to express NF2 isoforms 1 or isoform2 in a regulateable fashion.

Publications:

Scoles, D.R., Huynh, D.P. Chen, M.S., Burke, S.P., Gutmann, D.H. and Pulst, S.M. The Neurofibromatosis 2 tumor suppressor protein interacts with Hepatocyte Growth Factor-Regulated Tyrosine Kinase Substrate. Human Molecular Genetics 9:1567-1574;2000.

Gutmann, D.H., Haipiek, CA., Burk, S.P. Scoles, D.R., and Pulst, S.M. The NF2 interactor, hepatocyte growth factor-regulated tyrosine kinase substrate (HRS), associates with merlin in the "open" conformation and suppresses cell growth and motility. Human Molecular Genetics. 10:825-834;2001

Rui M. Costa, Tao Yang, Duong P. Huynh, Stefan M. Pulst, David H. Viskochil, Alcino J. Silva & Camilynn I. Brannan. Learning deficits, but normal development and tumor predisposition, in mice lacking exon 23a of Nf1. Nature genetics 27: 399-405; 2001

Publications in preparation:

Scoles, D.R., Chen, M.S., and Pulst, SM: Effects of NF2 missense mutations on Schwannomin Interactions. In Prep.

Scoles, D.R., Huynh, D.P. Gutmann, D.H., and Pulst, SM. The neurofibromatosis 2 tumor suppressor protein interaction with hepatocyte growth factor-regulated tyrosine kinase substrate (HRS) regulates STAT signaling and Schwann cell proliferation. In Prep.

Scoles, D.R., and Pulst, SM. Neurofibromatosis 2 (NF2) tumor suppressor schwannomin interacts with eIF3 p110 subunit. In Prep.

Numerous abstracts have been accepted and the research funded by DAMD has been presented as platform presentations at several national and international meetings.

Abstracts:

Scoles, D.R., Gutmann, D.H.G., Chen, M.S., Morrison, H., Huynh, D.P. and Pulst, SM. Neurofibromatosis 2 (NF2) tumor suppressor schwannomin interaction with HRS regulates STAT signaling and Schwann cell proliferation. *Neurology (suppl 3)* 54:A7 (2000).

Platform Presentations:

NF2 tumor suppressor schwannomin interaction with HRS regulates STAT signaling and Schwann cell proliferation. NNFF International Consortium for the Molecular Biology of NF1 and NF2, Aspen Colorado (2000)

Neurofibromatosis 2 (NF2) tumor suppressor schwannomin interaction with HRS regulates STAT signaling and Schwann cell proliferation 52nd American Academy of Neurology (2000)

Chairperson Scientific Sessions

Chair, Neurogenetics Section, AAN (2001)

Invited Lectures National

Case Studies in Neurogenetics American Academy of Neurology, Philadelphia, PA (2001)

Invited Lectures-International

2001 Annual ISONG Educational Conference, san Diego, CA (2001)

The *NF2* interactor, hepatocyte growth factor-regulated tyrosine kinase substrate (HRS), associates with merlin in the 'open' conformation and suppresses cell growth and motility

David H. Gutmann^{1,*}, Carrie A. Haipek¹, Stephen P. Burke¹, Chun-Xiao Sun¹, Daniel R. Scoles² and Stefan M. Pulst²

¹Department of Neurology, Washington University School of Medicine, Box 8111, 660 South Euclid Avenue, St Louis, MO 63110, USA and ²Division of Neurology, Cedars-Sinai Medical Center, Los Angeles, CA 90048, USA

Received 12 December 2000; Revised and Accepted 14 February 2001

The neurofibromatosis 2 tumor suppressor protein, merlin or schwannomin, functions as a negative growth regulator; however, its mechanism of action is not known. In an effort to determine how merlin regulates cell growth, we analyzed a recently identified novel merlin interactor, hepatocyte growth factor-regulated tyrosine kinase substrate (HRS). We demonstrate that regulated overexpression of HRS in rat schwannoma cells results in similar effects as overexpression of merlin, including growth inhibition, decreased motility and abnormalities in cell spreading. Previously, we showed that merlin forms an intramolecular association between the N- and C-termini and exists in 'open' and 'closed' conformations. Merlin interacts with HRS in the unfolded, or open, conformation. This HRS binding domain maps to merlin residues 453–557. Overexpression of C-terminal merlin has no effect on HRS function, arguing that merlin binding to HRS does not negatively regulate HRS growth suppressor activity. These results suggest the possibility that merlin and HRS may regulate cell growth in schwannoma cells through interacting pathways.

Introduction

Individuals affected with the inherited cancer predisposition syndrome, neurofibromatosis 2 (NF2), develop schwannomas and meningiomas with increased frequency (1). Because of this increased cancer risk, the *NF2* gene has been hypothesized to function as a tumor suppressor gene. Several observations support this idea. First, ependymomas, schwannomas and meningiomas from individuals with NF2 demonstrate homozygous inactivation of the *NF2* gene (2–5). In addition, nearly all sporadic schwannomas and 50–70% of sporadic meningiomas also demonstrate biallelic inactivation of the *NF2* gene, arguing that *NF2* functions as a critical growth regulator for these cells (6–8). Secondly, overexpression of

wild-type, but not mutant, *NF2* in schwannoma cell lines results in growth suppression (9–11). Thirdly, mice with a targeted mutation in the *Nf2* gene develop malignant tumors associated with inactivation of both copies of the *Nf2* gene (12).

The *NF2* gene was identified in 1993 by positional cloning, and was found to encode a protein termed schwannomin or merlin (13,14). Comparison of the predicted amino acid sequence of merlin demonstrated similarity with members of the Protein 4.1 family of protein and in particular three specific proteins, ezrin, radixin and moesin (ERM proteins) (15). Merlin is a 595 amino acid protein with three structural domains. The N-terminal domain (FERM domain), spanning residues 1–302, bears the greatest sequence conservation with the ERM proteins and is believed to mediate interactions with cell surface glycoproteins, like CD44 and intercellular adhesion molecules (ICAMs). The central domain (residues 303–478) contains a predicted α -helix, which is also found in ERM proteins. The C-terminal domain of merlin (residues 479–595) is unique and lacks the conventional actin-binding motif found in ERM proteins.

ERM proteins have been shown to form both homo- and heterotypic interactions by virtue of head (N-terminal) to tail (C-terminal) associations (16–18). These inter- and intramolecular associations have been postulated to regulate ERM activity. Previously, we have shown that merlin forms two intramolecular associations (10,19). One such interaction involves residues in the N-terminal domain, while the second interaction requires binding of the C-terminus of merlin to N-terminal domain residues (20,21). We have shown that the ability of merlin to form these productive intramolecular associations is critical to its ability to function as a growth regulator (10,19). Failure to form these associations impairs the ability of merlin to inhibit cell proliferation and motility (9,10,22).

Studies from a number of laboratories have demonstrated that overexpression of wild-type merlin, but not merlin containing *NF2* missense mutations, can inhibit cell proliferation (9,10,23). In addition to cell growth regulation, merlin also regulates actin cytoskeleton-mediated functions, such as spreading, motility and attachment. Previous studies from our laboratory have demonstrated that regulated merlin over-

*To whom correspondence should be addressed. Tel: +1 314 362 7149; Fax: +1 314 362 2388; Email: gutmannd@neuro.wustl.edu

expression dramatically reduces motility and disrupts the actin cytoskeleton during cell spreading (22). Antisense down-regulation of merlin also impairs cell attachment and increases cell proliferation (24). In addition, human schwannoma cells presumably lacking merlin expression have significant alterations in the actin cytoskeleton and in cell spreading (25), arguing that merlin may regulate intracellular pathways important for both growth and actin cytoskeleton processes.

In an effort to determine how merlin functions as a growth suppressor, several groups have employed yeast two-hybrid interaction cloning to identify novel merlin interactors (26–28). One such novel protein, hepatocyte growth factor (HGF)-regulated tyrosine kinase substrate (HRS) was recently identified (29). Since HGF is one of the most potent mitogens for Schwann cells and also promotes cell motility (30), we characterized HRS function with regard to the known properties of merlin. In this report, we demonstrate that HRS is a specific merlin interactor and that it associates with merlin via masked residues in the C-terminal domain of merlin. Moreover, we show that regulated HRS overexpression mimics the effect of merlin overexpression in rat schwannoma cells, suggesting that HRS is a good candidate for a merlin effector protein.

RESULTS

HRS uniquely binds to the C-terminus of merlin

Previously, we had demonstrated that HRS interacts with the C-terminus of merlin (29). In an effort to determine whether HRS is a specific merlin interacting protein, we performed *in vitro* glutathione *S*-transferase (GST) pull-down experiments to demonstrate that HRS does not interact with other ERM proteins. Whereas merlin binds to both full-length ezrin and radixin GST fusion proteins, we observed no binding of HRS to these two ERM proteins (Fig. 1A). Similar results were obtained with moesin (data not shown). To exclude the possibility that ERM intramolecular folding masked the ability of ezrin or radixin to bind HRS, we examined the binding of the C-termini of these proteins to associate with HRS *in vitro*. Using merlin–radixin hybrid proteins, we show that HRS only associates with the hybrid containing the C-terminus of merlin (radmer), but not the C-terminus of radixin (merad; Fig. 1B). Neither merad nor radmer can form intramolecular complexes, and they are unable to suppress schwannoma cell growth (9). The ability of merad to bind HRS suggests that the C-terminus of radixin lacks the residues required for HRS association, in contrast to radmer, which contains the C-terminus of merlin. Similar results were obtained with the C-terminus of ezrin (residues 284–585), which also fails to bind HRS (Fig. 1C). These results collectively suggest that HRS is a merlin-specific interacting protein and may be responsible for mediating merlin-specific functions.

To confirm that HRS binds to the C-terminus of merlin, we demonstrated that HRS associates with only the C-terminus (residues 299–595), but not the N-terminus (residues 1–302), of merlin (Fig. 1D). In addition, radmer contains merlin residues 341–595, thus narrowing the HRS binding domain to residues 341–579 of the full-length protein. This region is distinct from the binding domains reported for other merlin interacting proteins.

Regulated overexpression of HRS impairs cell proliferation and anchorage-independent growth

Previous experiments in our laboratory utilized zinc-inducible merlin expressing RT4 cell lines (22). Doxycycline regulatable RT4 cell lines (rtTA RT4 rat schwannoma cell lines) have since been generated by Helen Morrison (Karlsruhe, Germany) (31,32). To determine whether regulated overexpression of HRS had similar effects as merlin overexpression, we generated several RT4 rtTA cell lines expressing full-length HRS under the control of a doxycycline regulatable promoter. Two clones (3 and 10) were chosen for further study. As shown in Figure 2A, increased HRS expression is observed within 4 h of doxycycline treatment and peaks at 24 h. We determined the level of HRS overexpression to be 5–7-fold for each of the cell lines by scanning densitometry on separate western blots using the HRS Ab-1080-2 polyclonal antibody (data not shown).

As we had reported previously for merlin, regulated overexpression of HRS resulted in significant decreases in cell proliferation as determined by thymidine incorporation (Fig. 2B). We routinely observed a 1.7–2.7-fold decrease in thymidine incorporation as a result of HRS overexpression. No changes in cell death were noted by Trypan blue exclusion, FACS analysis or the TUNEL method for assessing apoptosis (data not shown). In addition to decreased cell proliferation, we observed a 1.8–2.7-fold decrease in anchorage-independent colony formation in response to HRS overexpression (Fig. 2C). Lastly, HRS overexpression reduced RT4 cell growth in a colony formation assay (Fig. 2D). These results argue that regulated overexpression of HRS results in growth inhibition.

Regulated overexpression of HRS results in abnormalities in cell spreading and motility

Previously, we had demonstrated that wild-type, but not mutant, merlin-regulated overexpression results in dramatic alterations in the actin cytoskeleton during cell attachment, as well as decreased cell motility (22). To determine whether HRS overexpression has similar effects on actin cytoskeleton-mediated processes, we assayed actin cytoskeleton organization upon cell attachment in RT4 cells induced to overexpress HRS. As shown in Figure 3A, doxycycline induction of HRS expression was associated with dramatic changes in the actin cytoskeleton as determined by phalloidin fluorescence cytometry. RT4 cells without HRS overexpression exhibit cortical actin rims at points of contact with the laminin substrate, whereas RT4 cells overexpressing HRS have a disorganized actin cytoskeleton and abnormal morphology. Similarly, HRS overexpression results in reduced cell motility assayed using a Boyden chamber as described in Materials and Methods (Fig. 3B). We routinely observed a 26–27% reduction in cell motility in this assay. The magnitude of the inhibition is similar to that observed for regulated merlin overexpression (data not shown).

HRS binds to merlin in the open conformation

Previous work from our laboratory and others has demonstrated that merlin, like other ERM proteins, exists in 'open' and 'closed' conformations dictated by the ability of merlin to form an intramolecular association between the N- and

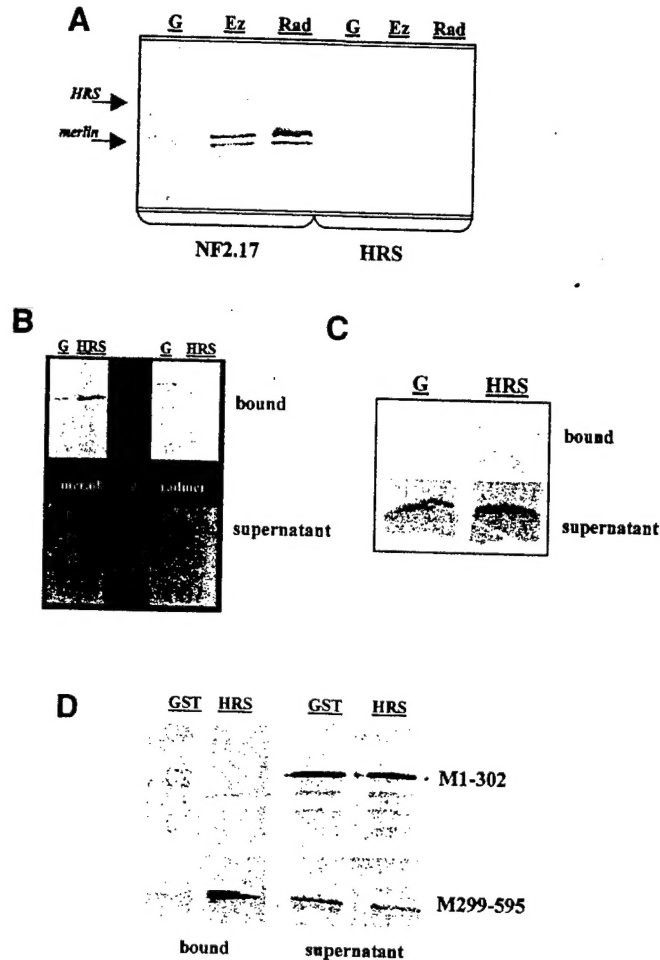


Figure 1. HRS interacts with the C-terminus of merlin *in vitro*. (A) HRS specifically interacts with merlin and not ezrin (Ez) or radixin (Rad). GST affinity chromatography pull-down experiments were performed with radiolabeled merlin (NF2.17) and HRS as described in Materials and Methods. No binding of merlin or HRS to the GST (G) beads alone was observed. Merlin bound to both ezrin and radixin, whereas no binding was observed with HRS. (B) HRS associates with the radmer, but not the merad, merlin–radixin hybrid. No binding was observed between either merlin–radixin hybrid or GST (G) alone. Whereas no binding was observed between HRS and merad (containing residues 1–340 of merlin), radmer (containing residues 341–595 of merlin) bound to HRS. The bound and supernatant fractions are shown. (C) HRS does not associate with the C-terminus (residues 284–595) of ezrin (ezrin C-term) *in vitro*. No binding was observed to GST (G) alone. The bound and supernatant fractions are shown. (D) HRS associates with the C-terminus of merlin. Radiolabeled N- (M1-302) and C-terminal (M299–595) fragments of merlin were interacted with GST alone (GST) or GST–HRS [full-length HRS (HRS)] as described in Materials and Methods. Whereas no binding was detected between N-terminal merlin and either GST or GST–HRS, the C-terminal fragment of merlin (residues 299–595; M299–595) binds specifically to GST–HRS and not GST alone.

C-termini of the protein (9,16,17,19–21). We further demonstrated that alterations in the extreme C-terminus of merlin impair the ability of the C-terminus to bind to N-terminal residues (e.g. merlin containing residues 1–568 and 1–557 or containing exon 16) (9). In addition, selected N-terminal domain mutations (e.g. L64P) also impair the ability of merlin to form a productive intramolecular association by disrupting the formation of an N-terminus self-association (19).

Initial experiments using the full-length merlin molecule failed to demonstrate significant binding to GST–HRS *in vitro* (Fig. 4A) and *in vivo* (Fig. 4B and C). This result is also reflected in a dramatic reduction in HRS binding using the yeast two-hybrid interaction system (29). Since merlin containing exon 16 (merlin isoform 2) was shown to strongly associate with HRS in the yeast two-hybrid system, we explored the possibility that HRS binding to merlin might be

unmasked in the open merlin conformation. To demonstrate this, we used the L64P NF2 missense mutant, which impairs the ability of merlin to form the N-terminal self-association required for merlin N-terminal:C-terminal folding (19). Whereas full-length wild-type merlin, which exists in the closed conformation, failed to bind significantly to HRS in this pull-down assay, the L64P merlin mutant demonstrated binding to HRS both *in vitro* and *in vivo* (Fig. 4A and C). These results suggest that merlin binding to HRS is partially masked by merlin self-association.

To further define the HRS binding domain within the C-terminus of merlin, we analyzed the ability of three additional laboratory-generated merlin deletion molecules. Merlin truncated at residue 568 (1–568) or 557 (1–557), or containing an internal deletion between residues 341 and 453 (Δ 342–452) were used in the *in vivo* interaction assay (Fig. 4B

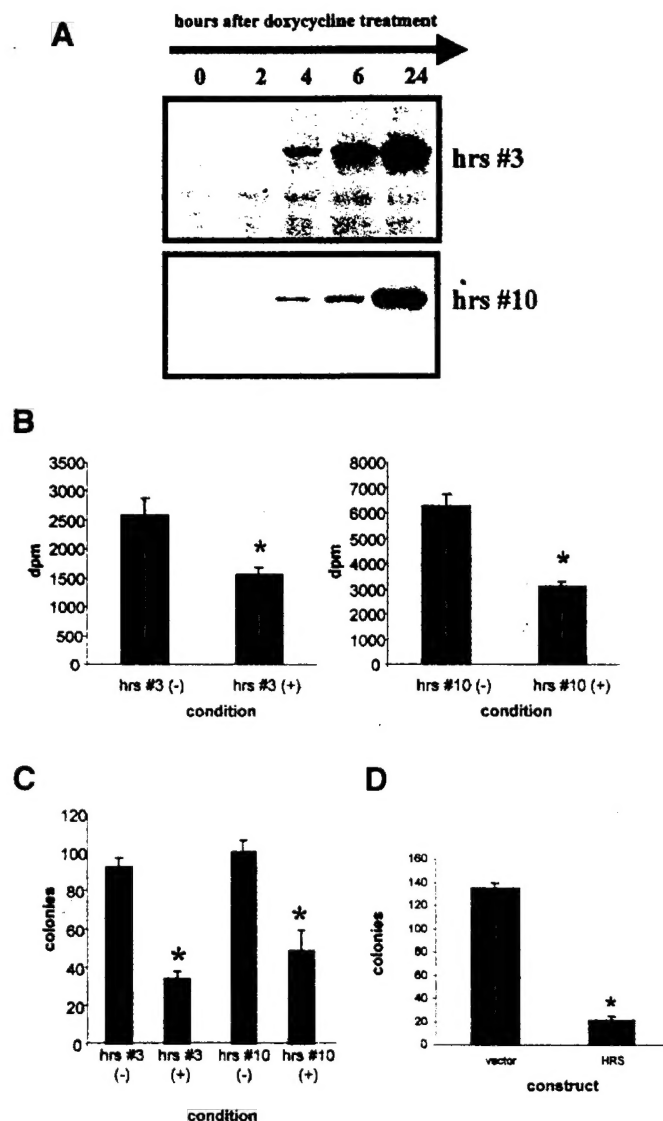


Figure 2. Regulated overexpression of HRS results in growth suppression. (A) RT4 rat schwannoma cells containing the rTA tetracycline transactivator were transfected with pUHD-10.3.HRS and two representative clones (3 and 10) were chosen for further study. Upon the addition of 1 μ g/ml doxycycline, an induction of HRS expression was seen over time. HRS was detected using the X-press antibody by western blot. (B) HRS induction results in a decrease in RT4 schwannoma cell proliferation in both HRS clones 3 and 10. Cell proliferation was measured using thymidine incorporation as described in Materials and Methods. There was 1.65–2.65-fold decrease in thymidine incorporation for cells expressing HRS compared with uninduced cells. (+) and (–) denote the addition or omission of doxycycline. The mean and standard deviation for each condition is shown. The asterisk denotes statistical significance using the Student's *t*-test ($P < 0.05$). (C) Soft agar growth assays were performed in quadruplicate as described in Materials and Methods. A 1.8–2.7-fold decrease was seen in the number of colonies in cells expressing HRS compared with uninduced cells. (+) and (–) denote the addition or omission of doxycycline. The mean and standard deviation for each condition is shown. The asterisk denotes statistical significance using the Student's *t*-test ($P < 0.05$). (D) Overexpression of HRS (pcDNA3.HRS) reduces RT4 cell colony formation after selection for 14 days in hygromycin compared to vector (pcDNA3) alone. The mean and standard deviation for each condition is shown. The asterisk denotes statistical significance using the Student's *t*-test ($P < 0.05$).

and C). Whereas wild-type merlin failed to interact with HRS, significant interactions were observed between all three merlin mutants and HRS. These results in combination with the

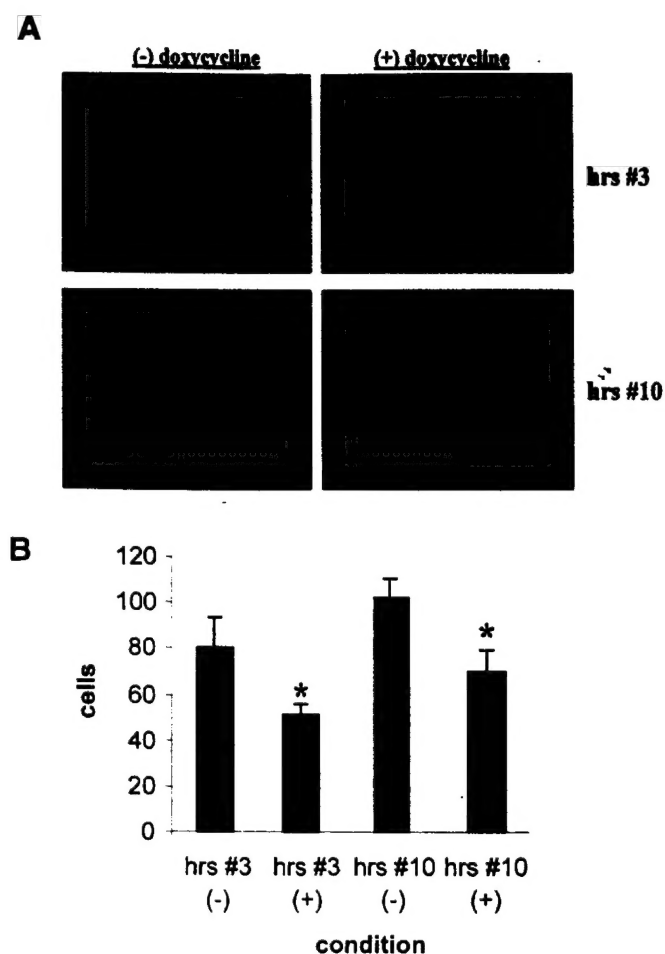


Figure 3. Regulated HRS overexpression impairs cell spreading and motility in RT4 schwannoma cells. (A) Induction of HRS was associated with abnormal spreading within 90 min of plating, as assessed using phalloidin-BODIPY immunofluorescence. Similar effects were observed for both HRS clone 3 and 10. No effect was observed with cell lines expressing the blank vector alone (data not shown). Photomicrographs were taken at 40 \times . Scale bar denotes 20 μ . (B) HRS RT4 cells were induced with doxycycline overnight and analyzed in a Boyden chamber motility assay as described in Materials and Methods. A reproducible 26–27% reduction in cell motility was observed after HRS overexpression in both RT4 clones. The mean and standard deviation for each condition is shown. (+) and (–) denote the addition or omission of doxycycline. Asterisks denote $P < 0.05$ using the Student's *t*-test.

merlin–radixin hybrid data narrow the HRS binding domain to between residues 453 and 557 in the C-terminus of merlin.

Merlin C-terminal domain binding to HRS does not impair HRS growth suppression

The fact that merlin binds to HRS in the open conformation suggested that the interaction of the C-terminus of merlin with HRS might regulate HRS function. To determine whether merlin C-terminal binding to HRS reduced the ability of HRS to inhibit cell proliferation, we generated RT4-regulated HRS-overexpressing clones that additionally constitutively overexpress the C-terminus of merlin (residues 299–595), either as the wild-type form, which binds HRS, or as the L535P mutant, which demonstrates reduced HRS binding in the yeast two-hybrid interaction system (29). As shown in Figure 5A, one

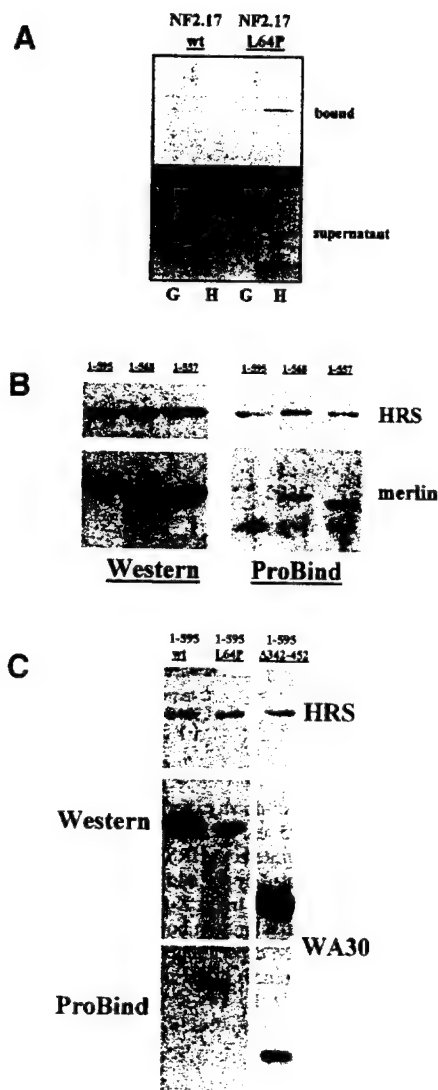


Figure 4. HRS binds to the unfolded merlin molecule. (A) GST affinity interaction experiments were performed using GST alone (G) or GST-HRS (H) as described in Materials and Methods. Whereas no binding of wild-type full-length merlin (NF2.17) to HRS was observed, full-length merlin containing the L64P mutation binds to HRS *in vitro*. No significant binding was observed to GST alone. The bound and supernatant fractions are shown for each interaction. (B) ProBind pull-down experiments were performed by transiently transfecting HRS clone 10 with various merlin expression constructs as described in Materials and Methods. Full-length merlin (1–595) or merlin truncated at residue 568 (1–568) or 557 (1–557) were transfected and the total protein was analyzed by western blot (Western) to demonstrate both HRS and merlin fragment expression (left panel). Lysates were incubated with ProBind resin and bound proteins eluted for SDS-PAGE and western blot using X-press and WA30 merlin antibodies (right panel). HRS was detected in all three eluates; however, only merlin truncated at residues 568 or 557 was bound to HRS. Full-length wild-type merlin did not bind HRS as shown *in vitro* in Figure 5A. (C) ProBind pull-down experiments were performed by transiently transfecting HRS clone 10 with merlin expression constructs as described in Materials and Methods. Full-length merlin (1–595) or merlin containing the L64P mutation (1–595 L64P) or missing residues 342–452 (1–595 Δ342–452) were transfected and the total protein was analyzed by western blot (Western) to demonstrate both HRS and merlin fragment expression (middle panel). Lysates were incubated with ProBind resin and bound proteins eluted for SDS-PAGE and western blot using X-press and WA30 merlin antibodies (upper and lower panels). HRS was detected in all three eluates; however, only merlin containing the L64P mutation or internally deleted of residues 342–452 bound to HRS. Full-length merlin containing the L64P mutation, but not wild-type merlin, bound HRS as shown *in vitro* in (A).

representative clone of each type demonstrate regulated HRS overexpression. The C-terminal no. 3 and L535P no. 5 clones additionally overexpress the wild-type and mutant C-terminal domains of merlin, respectively. The appearance of merlin C-terminal doublet bands (Fig. 5A) may represent phosphorylation of merlin (data not shown). To demonstrate that the C-terminus of merlin binds to HRS *in vivo*, pull-down experiments were performed using ProBind resin, which recovers the His-tagged HRS molecule, and eluates were analyzed for merlin C-terminus association. As shown in Figure 5B, the wild-type, but not the L535P mutant, merlin C-terminus binds HRS *in vivo*.

Thymidine incorporation experiments were next performed to analyze the effect of merlin C-terminus domain binding to HRS on HRS growth suppression. As shown in Figure 5C, no significant differences in growth suppression were observed between regulated HRS overexpressing clones containing wild-type or mutant merlin C-terminal domains compared with vector controls. These results argue that merlin C-terminal binding to HRS does not increase or impair the ability of HRS to regulate cell growth.

Although full-length merlin demonstrated reduced binding to HRS than the C-terminal construct alone, we explored the possibility that full-length merlin might interfere with HRS-mediated growth suppression. In these experiments, we used a doxycycline-regulatable merlin-expressing RT4 cell line (clone 6). Similar to our previous studies, regulatable overexpression of merlin resulted in increased merlin expression within 4–6 h of doxycycline treatment (Fig. 6A). Merlin induction is associated with a reduction in RT4 cell proliferation and anchorage-independent cell growth as determined by thymidine incorporation (Fig. 6B) and soft agar colony formation (Fig. 6C). No effect of doxycycline treatment on vector only containing cell lines was observed (C.A. Haipiek and D.H. Gutmann, unpublished data). The effect of HRS and merlin expression on RT4 cell growth was determined using a colony formation assay. Overexpression of either HRS or merlin results in reduced RT4 colony formation; however, co-expression of both HRS and merlin was associated with further reduction in growth suppression (Fig. 6D). These results argue that the full-length merlin does not interfere with HRS growth suppression.

Loss of merlin expression in sporadic meningiomas is not associated with reduced or absent HRS expression

Since merlin and HRS exhibit similar functions in RT4 cells, we explored the possibility that loss of merlin expression in tumors was coordinately associated with loss of HRS expression. We chose to examine seven sporadic meningiomas, since 50–60% of these tumors have bi-allelic *NF2* inactivation and lack merlin expression. In contrast, all sporadic schwannomas lack merlin expression, and correlations between HRS and merlin expression would not be possible. As shown in Figure 7, loss of merlin expression (tumors 2, 3 and 7) is not associated with loss of HRS expression. Moreover, in tumors where merlin expression was retained, the level of HRS expression did not correlate with the level of merlin expression (tumors 1, 4 and 6). These observations suggest that the presence of HRS alone is not sufficient to compensate for loss of merlin.

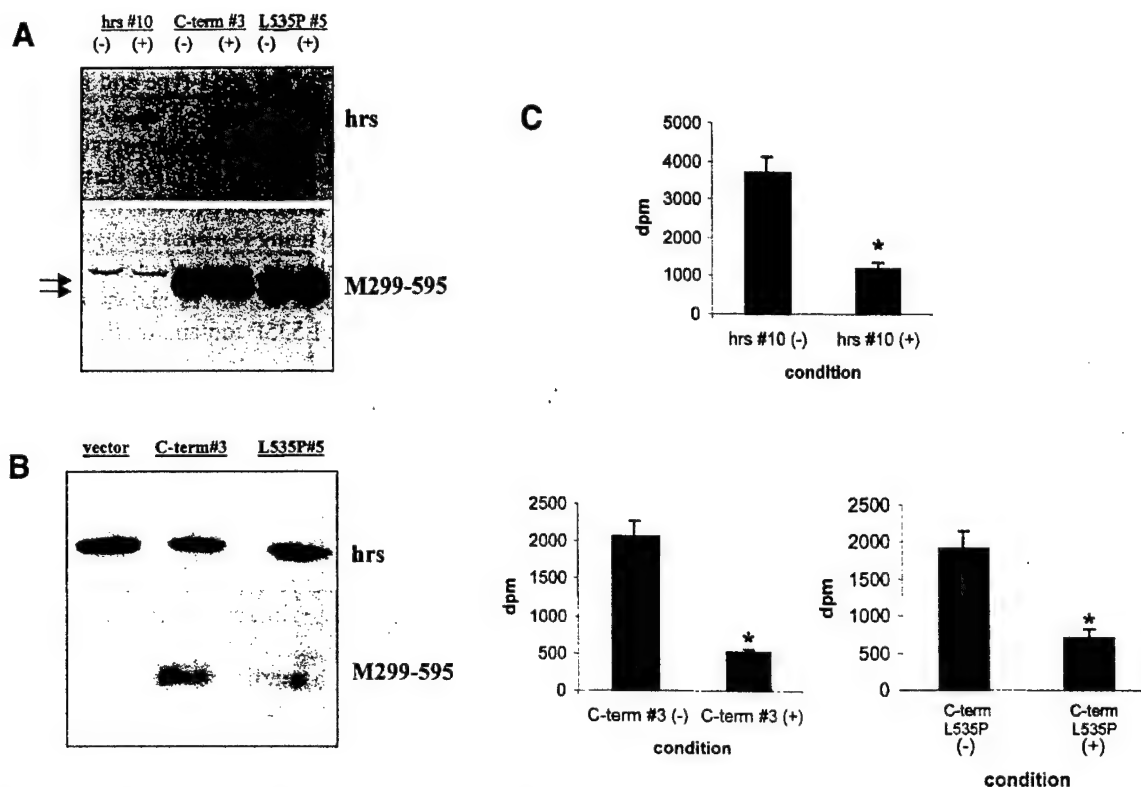


Figure 5. Overexpression of C-terminal merlin fragments does not impair HRS growth suppression. (A) ProBind pull-down experiments were performed by stably transfecting HRS clone 10 with merlin C-terminal expression constructs (wild-type C-terminus; residues 299–595 and C-terminal merlin containing the L535P mutation) as described in Materials and Methods. Total protein was analyzed by western blot (Western) to demonstrate both HRS and merlin C-terminal fragment (M299–595) expression. The merlin C-terminal fragment appears as a doublet (arrows). HRS expression is regulated by the addition of doxycycline, denoted by (+) and (–). (B) Lysates were incubated with ProBind resin and bound proteins eluted for SDS–PAGE and western blot using X-press and C18 merlin antibodies. Vector refers to HRS 10 transfected with pcDNA3 alone. HRS was detected in all three eluates. Wild-type C-terminal merlin bound HRS, however, significantly reduced binding was observed with C-terminal merlin containing the L535P mutation. (C) Thymidine incorporation experiments were performed as described in Materials and Methods. HRS-mediated growth suppression was observed in all three clones. No significant differences in the magnitude of growth suppression were observed between these RT4 cell lines.

DISCUSSION

HRS is a specific merlin interactor

Several merlin-interacting proteins have been reported over the past few years, including actin (33), β II-spectrin (28), CD44 (34), NHE-RF (sodium hydrogen exchange regulator factor) (21,27,35) and SCHIP-1 (26). To evaluate the ability of these interacting proteins as effectors of merlin growth suppressor function, we sought to determine whether potential merlin interactors specifically interact with merlin and display some of the functional properties attributed to merlin. In this report, we demonstrate that the merlin interacting protein, HRS (29), specifically interacts with merlin and not other ERM proteins, and also exhibits all of the functional properties we have previously attributed to merlin. Based on these data, we propose that HRS is an attractive candidate for a merlin effector protein relevant to *NF2* growth regulation.

The identification of HRS as a unique binding partner for merlin suggests that HRS might be involved in mediating merlin growth suppression. In this report, we demonstrate that HRS binds specifically to merlin and not to ERM proteins. HRS is expressed in the same tissues as merlin and associates with merlin both *in vitro* and *in vivo* (29). We define the HRS

binding domain in merlin to be between residues 453 and 557 using merlin–radixin hybrids and merlin truncation constructs. In support of this binding domain localization, HRS binding to merlin is dramatically impaired by a mutation at residue L535 that is contained within this domain (29). This HRS interaction region is distinct from the binding domains important for mediating merlin associations with NHE-RF (merlin residues 1–332) (21,35), SCHIP-1 (merlin residues 1–19 and 289–314) (26) and CD44 (merlin residues 1–300) (34), but overlaps partially with β II-spectrin binding domain (merlin residues 305–590) (28). Furthermore, this domain is located mostly within the predicted unique C-terminal domain of merlin (residues 479–595) which is not homologous to the C-terminus of other ERM proteins and is separate from the regions involved in merlin self-association, which involves residues 302–308 in the N-terminus and residues 579–595 in the C-terminus of merlin (19).

Merlin binds HRS in the open conformation

Previous work from our laboratory and others has suggested that merlin exists in open and closed conformations which may be important for mediating merlin function and associations (10,19–21,26). We have shown that the ability of merlin to func-

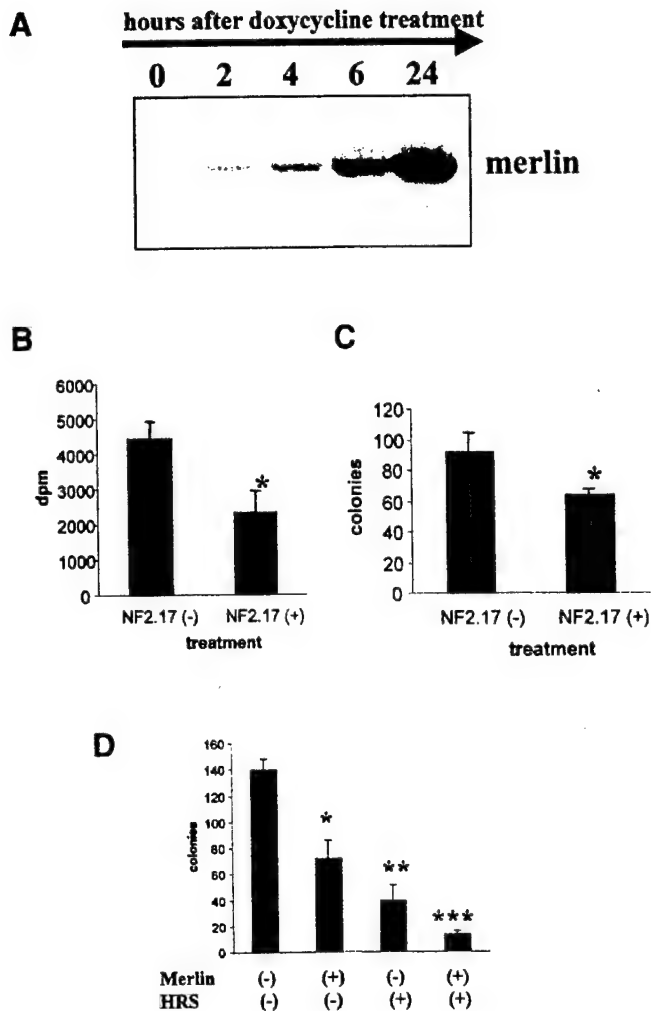


Figure 6. Regulated overexpression of merlin results in growth suppression. (A) RT4 rat schwannoma cells containing the rTA tetracycline transactivator were transfected with pUHD-10.3.NF2.17 and several clones were chosen for further study. One representative clone is shown (clone 6). Upon the addition of 1 µg/ml of doxycycline, an induction of merlin expression was seen over time. Merlin was detected using the WA30 polyclonal antibody by western blot. (B) Merlin induction results in a decrease in RT4 schwannoma cell proliferation. Cell proliferation was measured using thymidine incorporation as described in Materials and Methods. There was a 2-fold decrease in thymidine incorporation for cells expressing merlin compared with uninduced cells. (+) and (-) denote the addition or omission of doxycycline. The mean and standard deviation for each condition is shown. The asterisk denotes statistical significance using the Student's *t*-test ($P < 0.05$). (C) Soft agar growth assays were performed in quadruplicate as described in Materials and Methods. A 1.5-fold decrease in the number of colonies was seen in cells expressing merlin compared with uninduced cells. (+) and (-) denote the addition or omission of doxycycline. The mean and standard deviation for each condition is shown. The asterisk denotes statistical significance using the Student's *t*-test ($P < 0.05$). (D) Overexpression of HRS and merlin results in additive reductions in cell growth. RT4 cells inducibly expressing merlin (RT4 NF2.17 6) were transfected with pcDNA3 (-) or pcDNA3.HRS (+) in the HRS row in the presence or absence of doxycycline to induce merlin expression denoted by the (+) or (-) in the merlin row, respectively. Either merlin (condition 2) or HRS (condition 3) alone resulted in RT4 growth suppression. Expression of both merlin and HRS (condition 4) resulted in a further decrease in cell growth. The mean and standard deviation for each condition is shown. The single, double and triple asterisks denote statistical significance using the Student's *t*-test ($P < 0.05$) between each of the conditions.

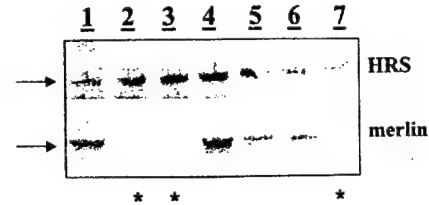


Figure 7. HRS and merlin expression are not coordinately expressed in sporadic human meningioma tumors. Seven sporadic human meningioma tumors were homogenized and equal amounts of total protein were separated by SDS-PAGE prior to immunoblotting with the Ab-1080-2 HRS and WA30 merlin antibodies. Three tumors (2, 3 and 7) have absent merlin expression (denoted by the asterisks), but retain HRS expression. No correlation between the level of merlin and HRS expression was seen in the four tumors with retained merlin expression (1, 4, 5 and 6).

tion as a growth regulator or impair actin cytoskeleton-mediated events is dependent on the formation of two intramolecular associations involving N-terminal:N-terminal as well as N terminal:C-terminal interactions. Recent reports have demonstrated that the ability of merlin to interact with NHE-RF and SCHIP-1 is also regulated by merlin intramolecular associations (21,26). Merlin appears to bind both of these interactors more avidly in the open conformation, suggesting that merlin folding might mask the SCHIP-1 and NHE-RF binding sites. Previously, we had shown that merlin isoform 2 containing the 'unfolded' exon 16 sequences bound HRS more strongly than the 'folded' merlin isoform 1 containing exon 17 sequences in a yeast two-hybrid interaction assay (29). In this report, we demonstrate that mutations that disrupt merlin self-association and result in a protein in the open conformation are able to bind HRS *in vitro*. This differential HRS association argues that merlin intramolecular associations might also influence HRS binding to merlin.

The ability of merlin to associate with HRS in the open conformation suggests that merlin/HRS function may be dictated by changes in the folding of merlin *in vivo*. Two events have been implicated in the regulation of merlin folding. These include the interaction of merlin with interacting proteins and the phosphorylation of merlin. It is possible that merlin binding to CD44 or NHE-RF permits merlin unfolding and allows for HRS binding. In this fashion, a productive merlin-CD44 interaction might result in growth suppression through binding to HRS. Alternatively, merlin is phosphorylated on serine and threonine residues (36) and the unphosphorylated form appears to be the predominant protein species under conditions when merlin is active. Support for this hypothesis also derives from experiments in which the unphosphorylated merlin preferentially associates with CD44 under conditions of confluency (31,32). It is possible that phosphorylation of merlin dictates which binding partners merlin associates with, and in that fashion, regulates cell growth regulation. Additional studies aimed at determining the significance of merlin phosphorylation to merlin function and protein interactions are required.

Regulated HRS and merlin overexpression impair similar cellular processes

For HRS to represent a reasonable candidate for a merlin effector protein, we sought to demonstrate that HRS and

merlin have similar functional properties. Using regulatable RT4 cell lines, we showed that HRS overexpression resulted in reduced cell proliferation and anchorage-independent cell growth as well as impaired actin cytoskeleton-associated events. Previous work from our laboratory demonstrated that regulated overexpression of wild-type, but not mutant, merlin molecules resulted in decreased cell proliferation as assayed by direct cell counting, thymidine incorporation and anchorage-independent cell growth (9,10,19). This growth suppression was not the result of decreased cell viability as determined by FACS analysis and TUNEL labeling. In addition, regulated overexpression of wild-type, but not mutant, merlin molecules resulted in reduced cell motility and attachment as well as dramatic alterations in the actin cytoskeleton during cell spreading. These results collectively support the notion that HRS might function similarly to merlin; however, further studies will be required to definitively prove this hypothesis.

Since merlin binds to HRS in the open conformation by virtue of C-terminal residues, we explored the possibility that binding to merlin could regulate HRS function. In these experiments, we found no effect of C-terminal merlin overexpression on HRS function. Similarly, we also found no evidence for impairment of merlin growth suppression by N-terminal (residues 1–480) or C-terminal (residues 480–777) HRS fragments (C.A. Haipek and D.H. Gutmann, unpublished results). These observations suggest that it is unlikely that HRS functions upstream of merlin and raise the possibility that either (i) HRS is downstream of merlin in a common growth inhibitory pathway; (ii) merlin and HRS coordinately regulate different upstream signaling cascades that converge on a common pathway to regulate cell growth and actin cytoskeleton-mediated processes; or (iii) HRS binding is required for proper merlin function and localization. Likewise, merlin binding to HRS could activate HRS, provide the proper subcellular localization required for HRS function or displace a different HRS binding protein to allow for HRS function.

Merlin and HRS are both expressed in cells that give rise to the tumors seen in individuals with NF2. Since merlin and HRS seem to mediate similar functions within the cell, it is possible that merlin loss is associated with coordinated HRS loss to result in absent merlin/HRS growth suppression. We excluded this possibility by western blot in sporadic meningiomas and demonstrated no correlation between merlin loss and HRS expression. It is therefore unlikely that retained HRS expression can compensate for merlin loss.

HRS represents an attractive candidate for a merlin effector protein. HRS is associated with the HGF signaling pathway, which has been implicated in both mitogenic and motogenic regulation in Schwann cells. HGF is one of the most potent growth factors for Schwann cell proliferation and motility (30). Since merlin regulates both growth and motility in Schwann cells, it is tempting to associate merlin with the HGF signaling pathway. Recent studies have demonstrated a link between HGF signaling and CD44 function. The HGF receptor, c-met, can stimulate HA production in a PI3-kinase-dependent fashion (37) as well as result in increased CD44 expression (38). In addition, HGF binds to a variant of CD44 (CD44v3) to promote c-met activation and MAPK activation (39). These results suggest that merlin may function as a critical growth regulator for Schwann cells by integrating the CD44 and HGF signaling pathways. Further studies specifically aimed at

relating CD44 and HGF signaling as well as establishing a direct connection between merlin and HRS growth suppression are presently underway.

MATERIALS AND METHODS

Antibodies, cDNA constructs and cell lines

The rabbit polyclonal antibodies that specifically recognize merlin (WA30) and HRS (ab-1080-2 and X-press tag) have been described previously (6,29). The merlin and HRS cDNAs used in these experiments were of human origin. N-terminal (M1–302), C-terminal (M299–595), merlin fragments containing residues 1–568 and 1–557 or deleted between residues 341 and 453 (Δ 342–452), merlin hybrids (merad and radmer), and missense merlin constructs have been described previously (9,19). The C-terminal ezrin construct was generated by cloning a *Bam*HI fragment of the full-length cDNA (residues 284–585) into pcDNA3.

HRS-expressing RT4 cell lines were established by transfecting RT4 cells containing the rTA reverse tetracycline transcriptional regulator (developed by H. Morrison) and puromycin resistance (pBABE.PURO) with pUHD10.3-HRS and pcDNA3 to confer G418 resistance (31,32). Several independent clones were selected in 500 μ g/ml G418 and 1 μ g/ml puromycin. Positive clones were screened for HRS expression using the X-press tag (Invitrogen) upon doxycycline addition, and two cell lines were maintained for further analysis (HRS clones 3 and 10). Additionally, wild-type merlin-expressing RT4 cell lines were generated and positive clones screened for regulatable merlin expression using WA30. Several clones were independently isolated and clone 6 is presented. A complete characterization of these wild-type and mutant merlin-regulatable RT4 cell lines will be presented elsewhere (D.H. Gutmann, A. Hirbe and C. Haipek, manuscript in preparation). RT4 cell lines transfected with pUHD-10.3 vector alone demonstrated no changes in cell proliferation, anchorage-independent growth, cell spreading and cell motility upon the addition of doxycycline.

Regulatable HRS RT4 schwannoma cell lines were also transfected with pcDNA3-C-term (residues 299–595) and C-term.L535P (residues 299–595 containing the L535P missense mutation) along with pCEP4 to confer hygromycin resistance. Clones were triply selected in G418, puromycin and hygromycin. Clones were selected that demonstrated regulatable HRS expression as well as constitutive C-terminal merlin expression using the Santa Cruz rabbit polyclonal antibody, C-18.

Thymidine incorporation, colony formation assay, TUNEL staining and growth in soft agar

Thymidine incorporation was performed as described previously on subconfluent cultures of RT4 schwannoma cells containing the doxycycline-regulatable HRS (clones 3 and 10) (9,10). For HRS induction, 1 μ g/ml doxycycline was added to the medium for 24 h while 1 μ Ci/ml tritiated thymidine was added for the last 4 h. Each condition (with or without doxycycline) was performed in six duplicate wells and cells were harvested in 0.2 M NaOH. Thymidine incorporation was measured on a scintillation counter and the mean and standard deviation determined for each condition.

The colony formation assay was performed by transfecting RT4 cells with equimolar amounts of pcDNA3 (vector), pcDNA3.NF2 (full-length containing exon 17) and pcDNA3.HRS (full-length residues 1–777). Cells were then selected in 200 µg/ml hygromycin for 14 days. Quadruplicate dishes for each transfection were counted after staining in 0.5% Crystal violet.

TUNEL labeling was performed using the Boehringer Mannheim *in situ* cell death (POD) detection kit according to the manufacturer's instructions, and visualized using a Nikon fluorescence microscope.

Soft agar growth assays were performed in quadruplicate either in the presence or absence of doxycycline. Briefly, 1000 RT4 cells were plated in 24-well plates with medium containing 0.3% Noble agar for 14–21 days. The number of colonies was determined by direct counting on an inverted microscope and the mean and standard deviation determined for each condition. Each experiment was repeated at least three times with identical results.

Cell spreading and motility

Glass coverslips were coated with 10 µg/ml of laminin (Sigma) in PBS overnight at 4°C. Coverslips were then aspirated. Inducible HRS RT4 cells, cultured in DMEM + 10% FBS were treated with 1 µg/ml doxycycline for 24 h, and then removed from dishes by trypsinization. Cells were washed twice in PBS, resuspended in DMEM + 10% FBS, with and without doxycycline, and plated onto the coverslips at ~100 000 cells/well. After 2 h, cells were fixed in 4% paraformaldehyde for 20 min at room temperature, permeabilized in PBS containing 0.1% Triton X-100, and stained with BODIPY-conjugated phalloidin (Molecular Probes, 0.2 U in 50 µl) for 20 min. Coverslips were then washed in PBS, mounted in 1 drop of Fluoromount G (EM Sciences), and examined on a Zeiss Axiophot microscope (22).

Cell motility was determined in Transwell chambers containing 8 µm membranes. Briefly, the bottom surface of the membrane was coated with Matrigel (Collaborative Research) and 10 000 cells were seeded on the outside of the chamber and allowed to attach for 1 h. Cells were gently washed and then the Transwells were inverted for 48 h either in the presence or absence of doxycycline at 37°C to allow for migration. Cells were then fixed in cold methanol for 30 min prior to staining with a LeukoStat staining kit (Fisher Scientific) and counted visually. The number of migrating cells was counted in quadruplicate and the mean and standard deviation determined for each condition. Each experiment was repeated at least three times with identical results.

HRS-merlin interaction *in vivo*

RT4 schwannoma cells with regulatable HRS expression and constitutive C-terminal merlin expression were lysed after a 24 h incubation in the presence or absence of doxycycline. Equal protein from these lysates was incubated with ProBind resin (Invitrogen) for 4 h followed by extensive washing in lysis buffer. Eluted proteins were separated by 10% SDS-PAGE and blotted with anti-merlin (C-18; Santa Cruz Biotechnology) and X-press tag antibodies to identify merlin C-terminal fragments and HRS, respectively. Total lysates were also separated by 10% SDS-PAGE for western blotting with the above antibodies.

In other experiments, merlin fragments cloned into pcDNA3 were transiently transfected into RT4 HRS clone 10 in the presence of doxycycline and lysed after 48 h. As above, equal protein from these lysates was incubated with ProBind resin (Invitrogen) for 4 h followed by extensive washing in lysis buffer. Eluted proteins were separated by 10% SDS-PAGE and blotted with anti-merlin (WA30) and X-press tag antibodies to identify merlin fragments and HRS, respectively. Total lysates were also separated by 10% SDS-PAGE for western blotting with the above antibodies. Each experiment was repeated at least three times with identical results.

GST fusion protein affinity chromatography

GST-merlin fusion proteins were generated as described previously (9,10,19). Briefly, GST, GST-merlin (M8-320), GST-ezrin, GST-moesin and GST-radixin were transformed into DE3 (BL21) competent cells for fusion protein production. The GST-ERM proteins were kindly provided by Dr Heinz Furthmayr (Stanford University). The GST-HRS construct was generated by PCR using primers that amplify the full-length protein (residues 1–777; HRS-F: 5'-GGATCCCC-ATGGGGCGAGGCAGC-3' and HRS-R: 5'-GTCAGTCGA-ATGAAATGAGCTGGGCCTC-3') and subcloned into pGEX.3X for fusion protein expression. Each construct was sequenced in its entirety and cloned into pGEX.3X for fusion protein production. Bacteria were induced overnight in 0.4 mM IPTG at room temperature and GST-merlin fusion proteins collected on glutathione-agarose beads (Sigma) for the interaction experiments.

GST fusion proteins were prepared as above for merlin interaction experiments with *in vitro* transcribed and translated merlin and HRS proteins, as described previously (9,10,19). *In vitro* transcribed and translated merlin proteins were synthesized in the presence of [³⁵S]methionine using the TnT protocol (Promega) according to the manufacturer's instructions and detected by autoradiography. In these experiments, radiolabeled proteins were incubated with equimolar amounts of GST fusion protein immobilized on glutathione-agarose beads for 4 h at 4°C. The unbound fraction was saved and the agarose beads were then washed four times in TEN buffer (10 mM Tris pH 7.5, 150 mM NaCl, 5 mM EDTA, 1% Triton X-100) and eluted in 1× Laemmli buffer. An equal fraction of the supernatant and eluted bound fraction was separated by SDS-PAGE and analyzed by autoradiography. In all experiments, no significant binding was observed with immobilized GST alone (<2% total bound). Each experiment has been repeated at least twice with identical results.

ACKNOWLEDGMENTS

We thank the members of our laboratories for their expert assistance during the execution of this project. This work was funded by grants from the National Institutes of Health (NS35848 to D.H.G., NS01428 to S.M.P. and NS10524 to D.R.S.) and the Department of Defense (DAMD-17-99-1-9548 to S.M.P.).

REFERENCES

1. Evans, D.G.R., Huson, S.M., Donnai, D., Neary, W., Blair, V., Newton, V., Strachan, T. and Harris, R. (1992) A genetic study of type 2 neurofibromatosis

- in the United Kingdom. II. Guidelines for genetic counseling. *J. Med. Genet.*, **29**, 847–852.
2. Merel, P., Hoang-Xuan, K., Sanson, M., Moreau-Aubry, A., Bijisma, E.K., Lazaro, C., Moisan, J.P., Resche, F., Nishisho, I., Estivill, X. *et al.* (1995) Predominant occurrence of somatic mutations of the *NF2* gene in meningiomas and schwannomas. *Genes Chromosomes Cancer*, **13**, 211–216.
 3. Ng, H.-k., Lau, K.-m., Tse, J.Y.M., Lo, K.-w., Wong, J.H.C., Poon, W.-s. and Huang, D.P. (1995) Combined molecular genetic studies of chromosome 22q and the neurofibromatosis type 2 gene in central nervous system tumors. *Neurosurgery*, **37**, 764–773.
 4. Rubio, M.-P., Correa, K.M., Ramesh, V., McCollin, M.M., Jacoby, L.B., von Deimling, A., Gusella, J.F. and Louis, D.N. (1994) Analysis of the neurofibromatosis 2 gene in human ependymomas and astrocytomas. *Cancer Res.*, **54**, 45–47.
 5. Twist, E.C., Rutledge, M.H., Rousseau, M., Sanson, M., Papi, L., Merel, P., Delattre, O., Thomas, G. and Rouleau, G.A. (1994) The neurofibromatosis type 2 gene is inactivated in schwannomas. *Hum. Mol. Genet.*, **3**, 147–151.
 6. Gutmann, D.H., Giordano, M.J., Fishback, A.S. and Guha, A. (1997) Loss of merlin expression in sporadic meningiomas, ependymomas and schwannomas. *Neurology*, **48**, 267–270.
 7. Lee, J.H., Sundaram, V., Stein, D.J., Kinney, S.E., Stacey, D.W. and Golubic, M. (1997) Reduced expression of schwannomin/merlin in human sporadic meningiomas. *Neurosurgery*, **40**, 578–587.
 8. Rutledge, M.H., Sarrazin, J., Rangaratnam, S., Phelan, C.M., Twist, E., Merel, P., Delattre, O., Thomas, G., Nordenskjold, M., Collins, V.P., Dumanski, J.P. and Rouleau, G.A. (1994) Evidence for the complete inactivation of the *NF2* gene in the majority of sporadic meningiomas. *Nature Genet.*, **6**, 180–184.
 9. Gutmann, D.H., Geist, R.T., Xu, H.M., Kim, J.S. and Saporito-Irwin, S. (1998) Defects in neurofibromatosis 2 protein function can arise at multiple levels. *Hum. Mol. Genet.*, **7**, 335–345.
 10. Sherman, L., Xu, H.M., Geist, R.T., Saporito-Irwin, S., Howells, N., Ponta, H., Herrlich, P. and Gutmann, D.H. (1997) Interdomain binding mediates tumor growth suppression by the *NF2* gene product. *Oncogene*, **15**, 2505–2509.
 11. Ikeda, K., Saeki, Y., Gonzalez-Agosti, C., Ramesh, V. and Chiocca, E.A. (1999) Inhibition of *NF2*-negative and *NF2*-positive primary human meningioma cell proliferation by overexpression of merlin due to vector-mediated gene transfer. *J. Neurosurg.*, **91**, 85–92.
 12. McClatchey, A.I., Saotome, I., Mercer, K., Crowley, D., Gusella, J.F., Bronson, R.T. and Jacks, T. (1998) Mice heterozygous for a mutation at the *Nf2* tumor suppressor locus develop a range of highly metastatic tumors. *Genes Dev.*, **12**, 1121–1133.
 13. Rouleau, G.A., Merel, P., Lutchman, M., Sanson, M., Zucman, J., Marineau, C., Hoang-Xuan, K., Demczuk, M., Desmaze, C., Plougastel, B. *et al.* (1993) Alteration in a new gene encoding a putative membrane-organizing protein causes neuro-fibromatosis type 2. *Nature*, **363**, 515–521.
 14. Trofatter, J.A., MacCollin, M.M., Rutter, J.L., Murrell, J.R., Duyao, M.P., Parry, D.M., Eldridge, R., Kley, N., Menon, A.G., Pulaski, K. *et al.* (1993) A novel moesin-, ezrin-, radixin-like gene is a candidate for the neurofibromatosis 2 tumor suppressor. *Cell*, **72**, 1–20.
 15. Tsukita, S., Oishi, K., Sato, N., Sagara, J., Kawai, A. and Tsukita, S. (1994) ERM family members as molecular linkers between the cell surface glycoprotein CD44 and actin-based cytoskeletons. *J. Cell Biol.*, **126**, 391–401.
 16. Gary, R. and Bretscher, A. (1993) Heterotypic and homotypic associations between ezrin and moesin, two putative membrane-cytoskeletal linking proteins. *Proc. Natl Acad. Sci. USA*, **90**, 10846–10850.
 17. Gary, R. and Bretscher, A. (1995) Ezrin self-association involves binding of an N-terminal domain to a normally masked C-terminal domain that includes the F-actin binding site. *Mol. Biol. Cell*, **6**, 1061–1075.
 18. Henry, M.D., Agosti, C.G. and Solomon, F. (1995) Molecular dissection of radixin: distinct and interdependent functions of the amino- and carboxy-terminal domains. *J. Cell Biol.*, **129**, 1007–1022.
 19. Gutmann, D.H., Haipke, C.A. and Lu, K.H. (1999) Neurofibromatosis 2 tumor suppressor protein, merlin, forms two functionally important intramolecular associations. *J. Neurosci. Res.*, **58**, 706–716.
 20. Meng, J.-J., Lowrie, D.J., Sun, H., Dorsey, E., Pelton, P.D., Bashour, A.-M., Groden, J., Ratner, N. and Ip, W. (2000) Interaction between two isoforms of the *NF2* tumor suppressor protein, merlin, and between merlin and ezrin, suggests modulation of ERM proteins by merlin. *J. Neurosci. Res.*, **62**, 491–502.
 21. Gonzalez-Agosti, C., Wiederhold, T., Herndon, M.E., Gusella, J. and Ramesh, V. (1999) Interdomain interaction of merlin isoforms and its influence on intermolecular binding to NHE-RF. *J. Biol. Chem.*, **274**, 34438–34442.
 22. Gutmann, D.H., Sherman, L., Seftor, L., Haipke, C., Lu, K.H. and Hendrix, M. (1999) Increased expression of the *NF2* tumor suppressor gene product, merlin, impairs cell motility, adhesion and spreading. *Hum. Mol. Genet.*, **8**, 267–275.
 23. Lutchman, M. and Rouleau, G.A. (1995) The neurofibromatosis type 2 gene product, schwannomin, suppresses growth of NIH 3T3 cells. *Cancer Res.*, **55**, 2270–2274.
 24. Huynh, D.P. and Pulst, S.-M. (1996) Neurofibromatosis 2 antisense oligodeoxynucleotides induce reversible inhibition of schwannomin synthesis and cell adhesion in STS26T and T98G cells. *Oncogene*, **13**, 73–84.
 25. Pelton, P.D., Sherman, L.S., Rizvi, T.A., Marchionni, M.A., Wood, P., Friedman, R.A. and Ratner, N. (1998) Ruffling membrane, stress fiber, cell spreading, and proliferation abnormalities in human schwannoma cells. *Oncogene*, **17**, 2195–2209.
 26. Gouttebroze, L., Brault, E., Muchardt, C., Camonis, J. and Thomas, G. (2000) Cloning and characterization of SCHIP-1, a novel protein interacting specifically with spliced isoforms and naturally occurring mutant *NF2* proteins. *Mol. Cell Biol.*, **20**, 1699–1712.
 27. Murthy, A., Gonzalez-Agosti, C., Cordero, E., Pinney, D., Candia, C., Solomon, F., Gusella, J. and Ramesh, V. (1998) NHE-RF, a regulatory cofactor for $\text{Na}^+\text{-H}^+$ exchange, is a common interactor for merlin and ERM (ERM) proteins. *J. Biol. Chem.*, **273**, 1273–1276.
 28. Scoles, D.R., Huynh, D.P., Coulsell, E.R., Robinson, N.G.G., Tamanoi, F. and Pulst, S.-M. (1996) The neurofibromatosis 2 gene product schwannomin interacts with beta-II-spectrin. *Nature Genet.*, **18**, 354–359.
 29. Scoles, D.R., Huynh, D.P., Chen, M.S., Burke, S.P., Gutmann, D.H. and Pulst, S.-M. (2000) The neurofibromatosis 2 tumor suppressor protein interacts with hepatocyte growth factor-regulated tyrosine kinase substrate. *Hum. Mol. Genet.*, **9**, 1567–1574.
 30. Krasnoselsky, A., Massay, M.J., DeFrances, M.C., Michalopoulos, G., Zarnegar, R. and Ratner, N. (1994) Hepatocyte growth factor is a mitogen for Schwann cells and is present in neurofibromas. *J. Neurosci.*, **14**, 7284–7290.
 31. Morrison, H., Sherman, L.S., Legg, J., Banine, F., Isacke, C., Haipke, C.A., Gutmann, D.H., Ponta, H. and Herrlich, P. (2001) The *NF2* tumor suppressor gene product, merlin, mediates contact inhibition of growth through interactions with CD44. *Genes Dev.*, in press.
 32. Herrlich, P., Morrison, H., Sleeman, J., Orian-Rousseau, V., Konig, H., Weg-Remers, S. and Ponta, H. (2000) CD44 acts as both a growth- and invasiveness-promoting molecule and as a tumor-suppressing cofactor. *Ann. N. Y. Acad. Sci.*, **910**, 106–120.
 33. Xu, H.M. and Gutmann, D.H. (1998) Merlin differentially associates with the microtubule and actin cytoskeleton. *J. Neurosci. Res.*, **51**, 403–415.
 34. Sainio, M., Zhao, F., Heiska, L., Turunen, O., den Bakker, M., Zwarthoff, E., Lutchman, M., Rouleau, G.A., Jaaskelainen, J., Vaheri, A. and Carpen, O. (1997) Neurofibromatosis 2 tumor suppressor protein co-localizes with ezrin and CD44 and associates with actin-containing cytoskeleton. *J. Cell Sci.*, **110**, 2249–2260.
 35. Reczek, D., Berryman, M. and Bretscher, A. (1997) Identification of EBP50: A PDZ-containing phosphoprotein that associates with members of the ezrin-radixin-moesin family. *J. Cell Biol.*, **139**, 169–179.
 36. Shaw, R.J., McClatchey, A.I. and Jacks, T. (1998) Regulation of the neurofibromatosis type 2 tumor suppressor protein, merlin, by adhesion and growth arrest stimulation. *J. Biol. Chem.*, **273**, 7757–7764.
 37. Kamikura, D.M., Khoury, H., Maroun, C., Naujokas, M.A. and Park, M. (2000) Enhanced transformation by a plasma membrane-associated met oncogene: activation of a phosphoinositide 3'-kinase-dependent autocrine loop involving hyaluronic acid and CD44. *Mol. Cell Biol.*, **20**, 3482–3296.
 38. Hiscox, S. and Jiang, W.G. (1997) Regulation of endothelial CD44 expression and endothelium-tumour cell interactions by hepatocyte growth factor/scatter factor. *Biochem. Biophys. Res. Commun.*, **233**, 1–5.
 39. van der Voort, R., Tahert, T.E.I., Wielenga, V.J.M., Spaargaren, M., Prevo, R., Smit, L., David, G., Hartmann, G., Gherardi, E. and Pals, S.T. (1999) Heparin sulfate-modified CD44 promotes hepatocyte growth factor/scatter factor-induced signal transduction through the receptor tyrosine kinase c-Met. *J. Biol. Chem.*, **274**, 6499–6506.

Learning deficits, but normal development and tumor predisposition, in mice lacking exon 23a of *Nf1*

Rui M. Costa^{1*}, Tao Yang^{2,5*}, Duong P. Huynh³, Stefan M. Pulst³, David H. Viskochil⁴, Alcino J. Silva¹ & Camilynn I. Brannan²

*These authors contributed equally to this work.

Neurofibromatosis type 1 (NF1) is a commonly inherited autosomal dominant disorder. Previous studies indicated that mice homozygous for a null mutation in *Nf1* exhibit mid-gestation lethality, whereas heterozygous mice have an increased predisposition to tumors and learning impairments. Here we show that mice lacking the alternatively spliced exon 23a, which modifies the GTPase-activating protein (GAP) domain of *Nf1*, are viable and physically normal, and do not have an increased tumor predisposition, but show specific learning impairments. Our findings have implications for the development of a treatment for the learning disabilities associated with NF1 and indicate that the GAP domain of NF1 modulates learning and memory.

Introduction

NF1 is a commonly inherited, autosomal dominant disorder that affects approximately 1 in 4,000 individuals. Mutations in the gene *NF1* cause several abnormalities in cell growth and tissue differentiation, including neurofibromas, café au lait spots and Lisch nodules of the iris^{1,2}. A broad range of learning disabilities are also associated with NF1 (ref. 3). The protein encoded by *NF1*, neurofibromin, contains a GAP domain, known to inhibit Ras-mediated signal transduction⁴⁻⁶. Previous studies showed that mice homozygous for a *Nf1* null mutation exhibit mid-gestational lethality, whereas heterozygous mice have an increased tumor predisposition and learning impairments⁷⁻⁹. It is therefore unclear whether the learning disabilities are associated with developmental abnormalities or increased tumor predisposition. An alternatively spliced *NF1* exon, 23a, encodes 63 bp within the GAP-related domain. Exclusion of exon 23a results in the type I isoform, whereas inclusion of 23a results in the type II isoform. The type II isoform has a greater affinity for Ras, but lower GAP activity than type I (refs. 10,11). To determine the role of the type II isoform, we developed a mouse strain specifically lacking exon 23a (*Nf1^{tm1Cbr}*, hereafter *Nf1^{23a-/-}*). We found that mice homozygous for this mutation (*Nf1^{23a-/-}*) are viable and physically normal, and do not have an increased tumor predisposition. *Nf1^{23a-/-}* mice, however, have specific learning impairments in hippocampal-dependent tasks (water maze and contextual discrimination) similar to those previously described for heterozygous null mutants⁹. These results demonstrate that the *Nf1* type II isoform is not required for either normal embryological development or tumor suppression, but is essential for normal brain function. Also, they indicate that the GAP-related domain of neurofibromin modulates learning and memory.

Results

Mice lacking exon 23a are viable and lack *Nf1* type II

We made the exon 23a deletion vector by joining a DNA fragment located upstream of *Nf1* exon 23a to a fragment 3' of exon 23a, generating a deletion of approximately 300 bp that included exon 23a (Fig. 1a). For positive selection of the targeting vector, a neomycin resistance cassette previously shown not to affect the transcription or splicing of the surrounding exons¹² was inserted in the deletion. After electroporation of the targeting vector and subsequent selection and screening of embryonic stem (ES) cell clones, 19 independent clones were identified that had the expected deletion of exon 23a.

Male chimeric mice were generated from two independent exon 23a deletion ES cell lines using standard procedures¹³. Upon maturity, males derived from each cell line were mated with C57BL/6J females, and germline transmission of the exon 23a deletion mutation was obtained from both lines. The resulting F₁ progeny were intercrossed to obtain F₂ mice of all three genotypes in the expected mendelian ratio. These (C57BL/6J×129/SvEv) F₂ animals were used in the experiments described below. Identical results were obtained from both independent lines; therefore, we combined them.

To confirm that the engineered mutation resulted in deletion of exon 23a, we used RT-PCR from RNA derived from brain tissue. We determined that the type II isoform was missing from *Nf1^{23a-/-}* animals, but present in *Nf1^{23a+/+}* and *Nf1^{23a+/-}* animals (Fig. 1b). Moreover, *Nf1^{23a-/-}* animals seemed to have normal levels of the type I isoform, indicating that the intronic neomycin resistance gene had no adverse affect on *Nf1* expression. Protein extracts prepared from brain tissue were analyzed by western-blot analysis using two affinity-purified

¹Departments of Neurobiology, Psychiatry and Psychology, BRI, UCLA, Los Angeles, California, USA. ²Department of Molecular Genetics and Microbiology, Center for Mammalian Genetics, and the University of Florida Brain Institute, University of Florida College of Medicine, Gainesville, Florida, USA. ³Cedars-Sinai Medical Center, UCLA School of Medicine, Los Angeles, California, USA. ⁴Division of Medical Genetics, University of Utah, Salt Lake City, Utah, USA. ⁵Present address: Brigham and Women's Hospital, Boston, Massachusetts, USA. Correspondence should be addressed to A.J.S. (e-mail: Silva@mednet.ucla.edu) or C.I.B. (e-mail: Brannan@mgm.ufl.edu).

anti-neurofibromin peptide antibodies¹⁴: NF1C, which recognizes the C terminus of neurofibromin; and GAP4, which recognizes the 21 amino acids encoded by exon 23a. We determined that, although all three genotypes express type I neurofibromin, only *Nf1*^{23a+/+} and *Nf1*^{23a+/-} mice express type II (Fig. 1c). These data demonstrate that the targeted deletion of *Nf1* exon 23a results in loss of type II neurofibromin. We then performed immunohistochemical analysis of brain tissue with the GAP4 antibody using *Nf1*^{23a-/-} tissue as a negative control for antibody specificity. In contrast to previous studies using RT-PCR analysis of mouse cortical cultures¹⁵, we found that type II neurofibromin is not only expressed in glia, but also in mature neurons in the mouse adult brain, including pyramidal neurons in the CA3 region of the hippocampus, Purkinje and granule cells in the cerebellum (Fig. 1d-i).

Nf1^{23a-/-} mice do not have increased predisposition for tumor formation

We analyzed 28 adult mice (between the ages of 4 and 13 months; average 8 months) at the histopathological level (13 *Nf1*^{23a-/-}, 10 *Nf1*^{23a+/-} and 5 *Nf1*^{23a+/+}). Complete examination revealed that only 4 of 28 mice had any abnormalities, but no abnormality was found more than once. One male *Nf1*^{23a-/-} mouse (8 months)

had an enlarged spleen (6 times normal) containing splenic hyperplasia with expansion of red pulp and increased extramedullary hematopoiesis. The lung, liver and kidneys revealed mild interstitial lymphocyte infiltrates. Another *Nf1*^{23a-/-} male (13 months) had a small liver adenoma (0.3 cm) and a small lung adenoma (0.3 cm). A *Nf1*^{23a-/-} female mouse (9 months) contained a large intra-abdominal cyst filled with yellow serous fluid. Microscopic examination revealed features consistent with endometriosis. Finally, a *Nf1*^{23a+/-} male (6.5 months) had an enlarged kidney (2 times normal), which on sectioning revealed multiple cystic lesions in the medulla and seemed to be a renal cystadenoma. The remaining 24 mice were found to be completely normal, indicating that there are neither obvious genotype-associated pathologies nor an increased risk for malignancy within the first year of life.

Examination of brain sections from all 28 mice stained with hematoxylin and eosin revealed no gross or microscopic abnormalities among the three genotypes. As there have been reports of astrogliosis in individuals with NF1 and in *Nf1*^{+/-} mice^{16,17}, we investigated the distribution of astrocytes in the brain by immunostaining with glial fibrillary acid protein (GFAP) antibody. Overall, no differences in the GFAP staining pattern or intensity were seen among the three groups of mice (data not shown).

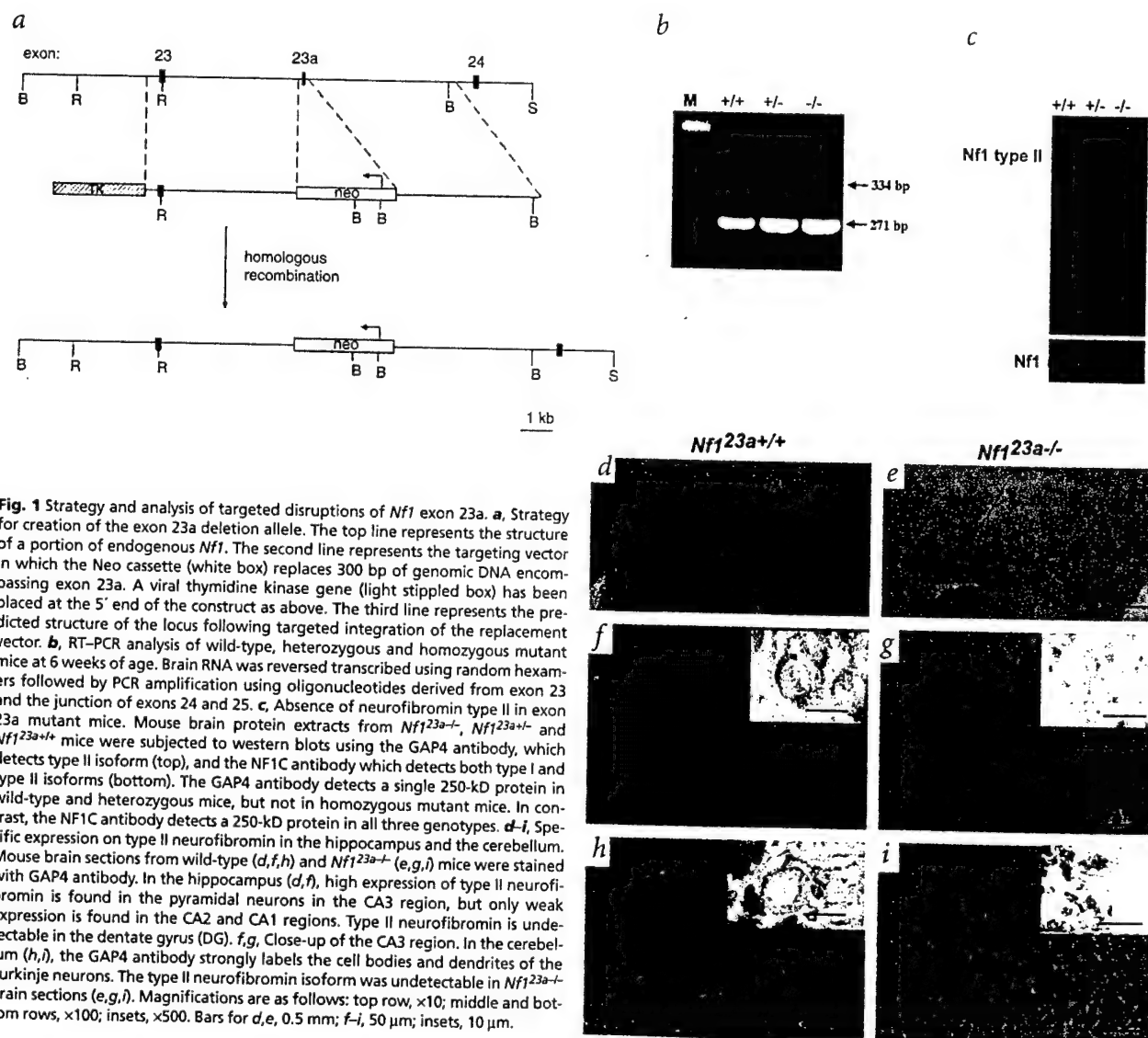


Fig. 1 Strategy and analysis of targeted disruptions of *Nf1* exon 23a. **a**, Strategy for creation of the exon 23a deletion allele. The top line represents the structure of a portion of endogenous *Nf1*. The second line represents the targeting vector in which the Neo cassette (white box) replaces 300 bp of genomic DNA encompassing exon 23a. A viral thymidine kinase gene (light stippled box) has been placed at the 5' end of the construct as above. The third line represents the predicted structure of the locus following targeted integration of the replacement vector. **b**, RT-PCR analysis of wild-type, heterozygous and homozygous mutant mice at 6 weeks of age. Brain RNA was reverse transcribed using random hexamers followed by PCR amplification using oligonucleotides derived from exon 23 and the junction of exons 24 and 25. **c**, Absence of neurofibromin type II in exon 23a mutant mice. Mouse brain protein extracts from *Nf1*^{23a-/-}, *Nf1*^{23a+/-} and *Nf1*^{23a+/+} mice were subjected to western blots using the GAP4 antibody, which detects type II isoform (top), and the NF1C antibody which detects both type I and type II isoforms (bottom). The GAP4 antibody detects a single 250-kD protein in wild-type and heterozygous mice, but not in homozygous mutant mice. In contrast, the NF1C antibody detects a 250-kD protein in all three genotypes. **d–i**, Specific expression on type II neurofibromin in the hippocampus and the cerebellum. Mouse brain sections from wild-type (**d**, **f**, **h**) and *Nf1*^{23a-/-} (**e**, **g**, **i**) mice were stained with GAP4 antibody. In the hippocampus (**d**, **f**), high expression of type II neurofibromin is found in the pyramidal neurons in the CA3 region, but only weak expression is found in the CA2 and CA1 regions. Type II neurofibromin is undetectable in the dentate gyrus (DG). **f**, **g**, Close-up of the CA3 region. In the cerebellum (**h**, **i**), the GAP4 antibody strongly labels the cell bodies and dendrites of the Purkinje neurons. The type II neurofibromin isoform was undetectable in *Nf1*^{23a-/-} brain sections (**e**, **g**, **i**). Magnifications are as follows: top row, $\times 10$; middle and bottom rows, $\times 100$; insets, $\times 500$. Bars for **d**, **e**, 0.5 mm; **f**–**i**, 50 μ m; insets, 10 μ m.

Because the *Nf1*^{+/-} mice have increased predisposition for tumor formation and lower survival rates than wild-type controls⁸, we aged another cohort of 27 mice (9 wild type, 10 *Nf1*^{23a+/-}, 8 *Nf1*^{23a-/-}) for over two years and analyzed their survival rates at different ages. No differences were observed in the survival rates of the different genotypes (Table 1; $\chi^2_6=2.27$, $P>0.05$). At the age of 27 months, the surviving mice were euthanized and necropsy was performed. One wild-type female had pus in the abdominal cavity with enlarged spleen and one *Nf1*^{23a-/-} male had a large (0.5 cm), well-confined mass in the prostate area, but no consistent pathology was seen among the three genotypes.

Spatial learning is impaired in *Nf1*^{23a-/-} mice

Visual-spatial problems are among the most common cognitive deficits detected in NF1 patients³ and previous results showed that *Nf1*^{+/-} mice have abnormal spatial learning⁹. To determine whether the *Nf1*^{23a-/-} mutation affected spatial learning, we tested these mice in the hidden version of the water maze, a task known to be sensitive to hippocampal lesions¹⁸. In this task an animal learns to locate a submerged platform in a pool filled with opaque water. During training, mice were given 2 trials per day for 14 days. No differences were observed between wild-type and mutant mice in floating, thigmotaxis behavior or swimming speed (wild type=19.9 cm/s, mutants=18.9, $F_{1,22}=0.297$, $P>0.05$). Across days, all animals decreased the time taken to find the platform ($F_{1,21}=13.914$, $P<0.05$) and no difference was found between *Nf1*^{23a-/-} mice and wild-type littermates ($F_{1,21}=2.548$, $P>0.05$; Fig. 2a). The time taken to find the platform during training is known to be a poor measure of spatial learning¹⁹. Therefore, we assessed spatial learning in probe trials in which the platform was removed from the pool. In a probe trial given after 10 days of training, the wild-type mice searched selectively,

Table 1 • Survival rates of the different genotypes

| Age (months) | 12 | 18 | 24 | 27 |
|------------------------------|------|-------|-----|-----|
| Genotype | | | | |
| wild type | 100% | 77% | 77% | 44% |
| <i>Nf1</i> ^{23a+/-} | 100% | 100% | 90% | 50% |
| <i>Nf1</i> ^{23a-/-} | 100% | 87.5% | 75% | 50% |

We aged 27 mice (9 wild type, 10 *Nf1*^{23a+/-} and 8 *Nf1*^{23a-/-}) to 27 months and analyzed their survival rates at different ages. No differences were observed in the survival rates of the different genotypes ($\chi^2_6=2.27$, $P>0.05$).

spending significantly more time searching for the platform in the quadrant where the platform was during training than in the other quadrants ($F_{3,44}=12.242$, $P<0.05$), whereas *Nf1*^{23a-/-} mice searched randomly ($F_{3,44}=2.716$, $P>0.05$) and spent significantly less time searching for the platform in the training quadrant than wild type ($F_{3,22}=6.555$, $P<0.05$; Fig. 2c). Using another very sensitive measure to assess spatial learning²⁰ (proximity to platform), we verified that wild-type mice searched on average closer to the exact platform position than to the symmetrically opposite position in the pool ($t_{11}=-2.612$, $P<0.05$), whereas mutants did not ($t_{11}=0.709$, $P>0.05$; Fig. 2e).

Previous studies showed that additional training alleviates the learning deficits in the *Nf1*^{+/-} mice⁹. Consistently, following four additional days of training, the *Nf1*^{23a-/-} mice searched as selectively as wild-type controls in a probe test ($F=1.301$, $P>0.05$; Fig. 3d). They spent significantly more time searching in the training quadrant than in the other quadrants ($F_{3,44}=15.348$, $P<0.05$) and searched closer to the exact platform position ($t_{11}=-2.905$, $P<0.05$; Fig. 3f).

To determine whether deficits in motivation, motor coordination, or vision account for the abnormalities in spatial learning,

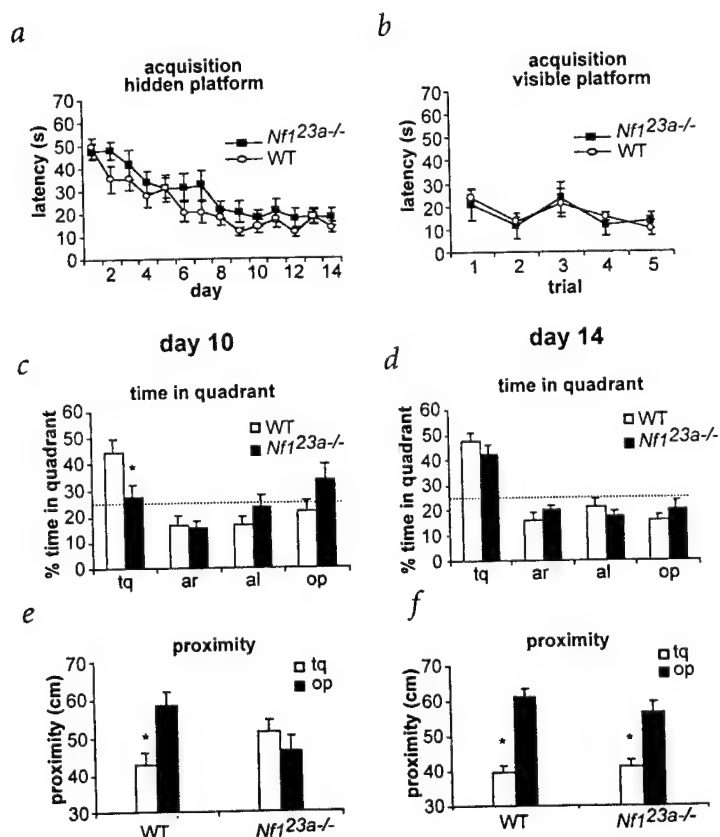
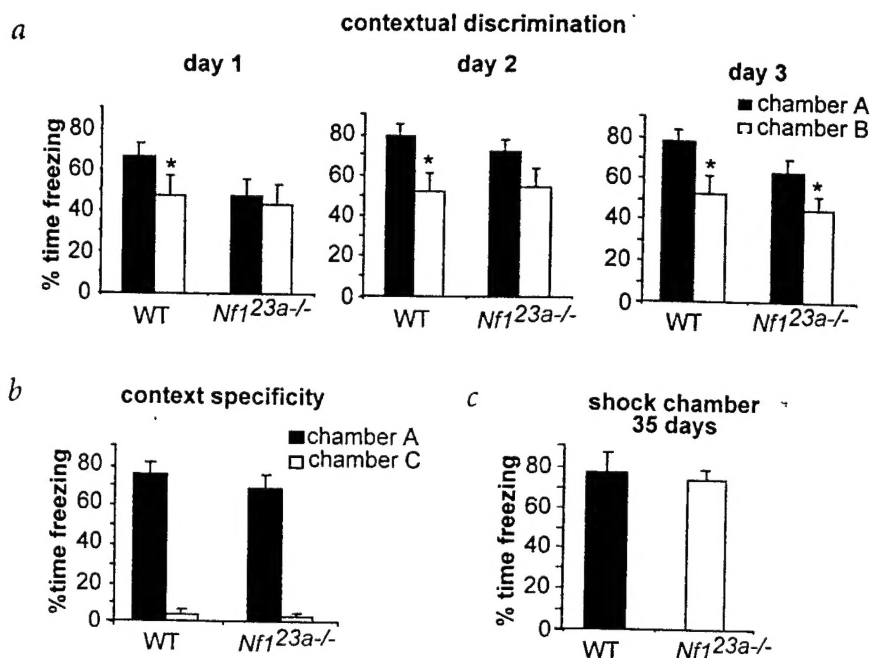


Fig. 2 Spatial learning in the water maze. **a**, *Nf1*^{23a-/-} mice ($n=12$) and wild-type littermates ($n=12$) were trained for 14 d, with 2 trials per day in the water maze. The average latency to reach the hidden platform is plotted. Escape latencies decrease across days ($F_{1,21}=13.914$, $P<0.05$) and there is no difference in latencies between mutants and controls during training ($F_{1,21}=2.548$, $P>0.05$). **b**, After the hidden version of the water maze, the animals were run in the visible platform task. There was no difference in latency to get to the platform across trials between wild-type and mutants ($F_{1,14}=0.30$, $P>0.05$). **c**, Results of a probe trial given after 10 days of training. The percentage of time animals spent searching in each of the training quadrants is shown. ANOVA shows that there is an effect of percentage time spent in quadrant for wild type ($F_{3,44}=12.242$, $P<0.05$). Post-hoc analysis show that wild-type mice spent significantly more time searching in the training quadrant than in any of the other quadrants (Fisher PLSD, $P<0.05$). Mutants did not search selectively in any of the quadrants ($F_{3,44}=2.716$, $P>0.05$) and spent significantly less time searching in the training quadrant than wild type ($F_{3,22}=6.555$, $P<0.05$). **d**, Probe trial given after 14 days of training. Both mutants ($F_{3,44}=15.348$, $P<0.05$) and wild type ($F_{3,44}=23.110$, $P<0.05$) searched selectively and spent significantly more time searching in the training quadrant than in any of the other quadrants (Fisher PLSD, $P<0.05$). **e**, During the probe trial given at day 10, wild-type mice searched on average closer to the exact position of the platform during training than to the symmetric position in the opposite quadrant ($t_{11}=-2.612$, $P<0.05$), whereas mutants did not ($t_{11}=0.709$, $P>0.05$). **f**, Probe trial day 14. Both mutants and wild type searched on average closer to the exact platform position than to the opposite position in the pool ($t_{11}=-2.905$, $P<0.05$; $t_{11}=-6.71$, $P<0.05$). Dashed line indicates random search (25% in each quadrant). *Significant difference, $P<0.05$. tq, training quadrant; ar, adjacent right quadrant; al, adjacent left quadrant; op, opposite quadrant.

Fig. 3 Contextual discrimination. **a**, Percentage of time spent freezing in chamber A (shock context, filled bars) versus chamber B (no-shock context, open bars) shown for each of the three testing days. Wild-type mice spent significantly more time freezing in the chamber where they were shocked than in the other chamber on each test day (day 1, $A=66.8$, $B=47.4$, $t_8=2.407$, $P<0.05$; day 2 $A=78.0$, $B=51.2$, $t_8=5.873$, $P<0.05$; day 3, $A=77.2$, $B=52.2$, $t_8=4.890$, $P<0.05$), showing that they discriminate between the two chambers. $Nf1^{23a/-}$ mutants did not discriminate between the chambers (day 1, $A=47.5$, $B=43.3$, $t_8=0.603$, $P>0.05$; day 2, $A=70.5$, $B=53.5$, $t_8=1.839$, $P>0.05$) during the first two days of training, but they finally discriminated after three days of training ($A=62.4$, $B=44.8$, $t_8=2.534$, $P<0.05$). **b**, Specificity of the conditioned freezing. After training in contexts A and B, mutants and wild-type mice were tested in chamber A and a novel chamber, C. Both mutants ($A=66.6$, $C=3.1$) and wild-type ($A=73.7$, $C=3.8$) showed similarly robust freezing in chamber A (shock context, black bars, $F_{1,15}=0.637$, $P>0.05$) and essentially no freezing in chamber C (novel context, gray bars, $F_{1,15}=0.111$, $P>0.05$). **c**, Memory consolidation does not seem to be impaired in the mutants because both mutant (open bars) and wild-type controls (filled bars) exhibited similar levels of freezing (wild type=77.1, mutants=73.5, $F_{1,15}=0.111$, $P>0.05$) when re-exposed 35 days later to the same chamber where they were shocked. *Significant difference, $P<0.05$.



the same animals were tested in the visible platform version of the water maze, a task that is not affected by hippocampal lesions¹⁸. In this task, animals must locate a platform marked with a visible cue. Both mutant and wild-type control mice acquired the task similarly, as the times taken to reach the visible platform were not different between the groups ($F_{1,14}=0.030$, $P>0.05$, Fig. 3b).

$Nf1^{23a/-}$ mice are impaired in contextual discrimination

We confirmed the water maze results using another hippocampal-dependent task, contextual discrimination²¹. In this task animals are required to discriminate between two similar chambers, one in which they receive a mild foot shock (chamber A) and another in which they do not (chamber B). Contextual discrimination is assessed by measuring the time spent 'freezing' (that is, without any bodily movement aside from respiration) in each chamber. Throughout training, wild-type mice froze significantly more in the chamber where they were shocked than in the other chamber ($P<0.05$ for all three days), showing that they discriminate between the two chambers (Fig. 3a). In contrast, during the first two days of training, $Nf1^{23a/-}$ mutants did not discriminate between the chambers ($P>0.05$ for both days). $Nf1^{23a/-}$ mice finally discriminated between the chambers after three days of training (day 3, $t_8=-2.534$, $P<0.05$), confirming that, just as with spatial learning, additional training can overcome the learning deficits. When tested in chamber C, which is very different from the training chambers, both wild-type and mutant mice showed little or no freezing (Fig. 3b). This demonstrates that the freezing responses in chamber B are probably triggered by the cues shared with chamber A. The $Nf1^{23a/-}$ mutation does not seem to affect long-term memory, because mutants and controls had similar levels of freezing ($F_{1,15}=0.111$, $P>0.05$) when tested 35 days after training (Fig. 3c). Also, the ability to freeze seems to be unaffected by the mutation. In chamber A, both baseline freezing (wild type, 9.0; $Nf1^{23a/-}$, 6.7; $F_{1,15}=0.264$, $P>0.05$) and freezing after foot-shock delivery ($F_{1,15}=3.495$, $P>0.05$) were similar between wild type and mutants.

$Nf1^{23a/-}$ mice have delayed acquisition of motor skills

Some individuals with NF1 show delayed acquisition of motor skills and motor coordination problems³. To determine whether the $Nf1^{23a/-}$ mutation affects motor function, we tested the mice on an accelerating rota-rod^{22,23} (4–40 r.p.m. in 300 s). $Nf1^{23a/-}$ mice fell off the rotating rod sooner than wild-type mice ($F_{1,17}=4.84$, $P<0.05$; Fig. 4a). This motor coordination impairment is not due to greater fatigue in the mutants because, at an intermediate, constant speed (14 r.p.m.), mutants and controls showed no differences in latency to fall from the rotating rod ($F_{1,16}=0.262$, $P>0.05$; Fig. 4b).

The effects of the $Nf1^{23a/-}$ mutation are specific

It is unlikely that the learning deficits in these mice are caused by generalized neurological problems or poor motor performance, as swimming speed, ability to freeze, ambulation (hind paw analysis²³), exploratory behavior (open field²³), muscular strength (wire hang²⁴) and body weight (data not shown) were not affected by the mutation.

Just as NF1 patients do not show learning deficits in all tasks, the $Nf1^{23a/-}$ mutation did not affect all forms of learning. When tested in the social transmission of food preferences²⁵, a task that assesses the capability of an animal to remember a food smelled in the breath of a littermate, $Nf1^{23a/-}$ mice learned as well as wild-type controls ($t_8=3.23$, $P<0.05$; Fig. 5). This is relevant because the brain regions required to solve this task²⁶ are different from the ones required for the water maze¹⁸ and contextual discrimination²¹, revealing that the effects of this mutation are specific.

Discussion

Neurofibromin is a complex protein that is implicated in a number of biological processes, including growth, differentiation, learning and memory. Accordingly, inactivating mutations of *NF1* in humans and mice results in a wide spectrum of symptoms ranging from increased tumor predisposition to learning disabilities²⁷. *NF1* encodes several distinct isoforms of neurofibromin.

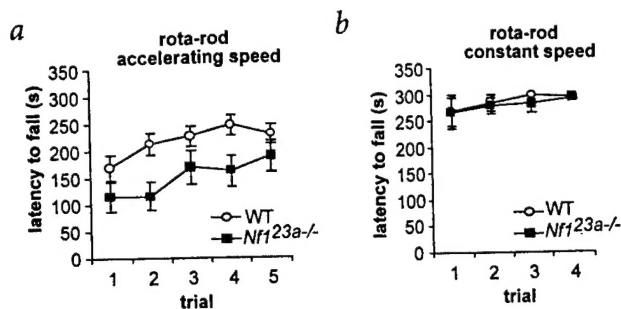


Fig. 4 Motor performance in the rota-rod. **a**, Accelerating rota-rod. Wild-type and *Nf1*^{23a-/-} were given 5 trials in an accelerating rota-rod (4–40 r.p.m. in 5 min) during 1 day. All subjects showed an increase in the latency to fall across trials ($F_{1,17}=13.3$, $P<0.05$) indicating that they improved their performance across trials. In average mutants fell off the rotating rod sooner than the wild type ($F_{1,17}=4.84$, $P<0.05$). **b**, Constant speed rota-rod. The mice were given four trials at a lower constant speed (14 r.p.m. for 5 min) during one day. Under these conditions, mutants and controls showed no differences in latency to fall from the rotating rod ($F_{1,16}=0.262$, $P>0.05$).

Here we have demonstrated that one isoform, type II, is important for brain function, but not for embryological development or tumor suppression. It is possible that other alternatively spliced exons (such as exon 9a) expressed postnatally in forebrain neurons²⁸, also have a role in mechanisms underlying learning and memory. Our data indicate that the learning deficits caused by mutations that inactivate *NF1* in mice and humans are not a result of developmental deficits or undetected tumors. Instead, they suggest that the learning deficits in individuals with *NF1* are caused by the disruption of neurofibromin function in the adult brain, a finding with important implications for the development of a treatment for the learning disabilities associated with *NF1*.

Exon 23a modifies the GAP domain of *NF1*. Thus, our results indicate that modulation of the Ras pathway is important to learning and memory. These data are consistent with previous findings. First, patients carrying a missense mutation that specifically eliminates the Ras-GAP activity of neurofibromin have learning disabilities²⁹. Second, pharmacological disruption of the downstream Ras target MAPK disrupts learning in rodents³⁰. Third, a deletion mutation of Ras guanine-nucleotide-exchange factor (Ras-GRF) also affects learning and memory in mice³¹. In addition, *Nf1*-null mutations are known to elevate Ras-GTP (refs. 32,33), and cause learning disabilities⁹. These results suggest that either abnormally high or low Ras-GTP levels affect learning and memory. It has been shown that type I neurofibromin has higher GAP activity and lower affinity for Ras than type II (refs. 10,11), offering the possibility that the ratio between

the two isoforms modulates Ras signaling. Because *Nf1* type I and type II isoforms are expressed in some of the same populations of cells in the adult brain, and the relative expression of these two isoforms in neuronal cultures is subject to modulation by extrinsic factors, such as NGF (ref. 34), we propose that differential expression of these two isoforms may have a role in fine-tuning Ras activity in the central nervous system.

Although the neurological and cognitive deficits associated with *NF1* are pleiomorphic and incompletely penetrant (only about half of individuals show learning disabilities), spatial problems are the most common abnormality associated with this condition. Although it is unclear whether the same brain systems underlie the spatial phenotype in mice and humans, it is important to note that both the heterozygous null *Nf1* mutation and the *Nf1*^{23a-/-} mutation primarily result in incompletely penetrant spatial learning deficits in mice. Additionally, *NF1* mutations can result in motor coordination problems in both mice and humans. These compelling parallels demonstrate the usefulness of mouse models to understand the etiology of learning deficits in *NF1*.

Methods

Targeted deletion of exon 23a. The exon 23a deletion vector was made by joining a 5' upstream 4.8 kb *BsrFI* fragment containing exon 23 to a 3' downstream 4.6 kb *BstBI*-(*NotI*) fragment containing intronic sequence. This resulted in a deletion of approximately 300 bp of genomic DNA, which included exon 23a. A neomycin selectable marker (KT3NP4) was inserted between the two fragments in the opposite transcriptional orientation relative to *Nf1* and a PGK-TK cassette was placed at the 5' end of the construct. CJ.7 cells³⁵ were cultured and electroporated with linearized vector using standard conditions³⁶, and then plated onto gelatin coated dishes in media containing ESGRO (1,000 μ M; Gibco BRL). After 24 h, the culture medium was changed to include 250 μ g/ml active concentration of Geneticin (Gibco BRL). After 48 h it was changed again to include 0.7 μ M FIAU (0.7 μ M; Oclassen Pharmaceuticals). Seven days after electroporation, 500 Geneticin- and FIAU-resistant colonies were picked and expanded on mouse embryo fibroblasts in the presence of Geneticin. We isolated genomic DNA from ES cells as described³⁷. Aliquots of the DNA (5 μ g) were digested to completion with *Bam*HI, then electrophoresed through 0.8% agarose gels, transferred to Hybond nylon membranes (Amersham) and subsequently screened using a 0.5-kb *EcoRI*-*SpeI* fragment mapping 5' to the limit of homology. Autoradiography was carried out at -70 °C using Kodak XAR film. We found the expected replacement event in 1 of every 9 clones. We selected two independent clones to derive chimeric mice according to standard procedures¹³.

RT-PCR. We pretreated total brain RNA (10 μ g) with DNase I (Gibco BRL). Half of the reaction was subsequently used to synthesize first-strand cDNA with Superscript II reverse transcriptase (Gibco BRL) and random primers (Gibco BRL). The other half of the reaction was manipulated in parallel in the absence of RT. We used one-twentieth of the +RT or -RT reactions to program PCR reactions using the following conditions: 10 mM Tris-HCl, pH 8.3, 50 mM KCl, 1.5 mM MgCl₂, 0.125 mM of the four dNTPs, 1 unit *Taq* DNA polymerase (Boehringer) and 4 μ M each of the primers 5'-GCGGAACCTCCTTCAGATGACTG-3' and 5'-GCTCTGAAGTACCTTTGAC-3'. PCR amplification conditions were as follows: 95 °C for 4 min, followed by 40 cycles of 94 °C for 1 min, 55 °C for 1 min, and 72 °C for 2 min. The final cycle was followed by a 10-min extension period at 72 °C.

Genotyping. To genotype genomic DNA isolated from the exon 23a deletion mice, we used three oligonucleotide primers: *Nf23a*,

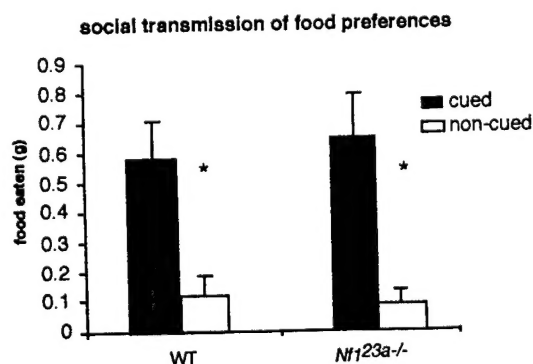


Fig. 5 Social transmission of food preferences. After 15 min of interaction with demonstrator mice, both wild-type and mutant mice showed robust socially transmitted food preference (wild type, cued=0.58 g, non-cued=0.12 g, $t_8=3.16$, $P<0.05$; *Nf1*^{23a-/-}, cued=0.65 g, non-cued=0.09 g, $t_8=3.23$, $P<0.05$). Even with shorter interaction times (5 min), no differences were observed between mutant and wild-type mice (data not shown).

5'-GCAACTTGCCACTCCCTACTGAATAAGCTACAGTAAAA-3'; intron 23a, 5'-CCACTCACATGACCCGCAACG-3'; and KT3NP4, 5'-GGAGTTGTTGACGCTAGGGCTC-3'. PCR conditions were the same as above except of the following changes: 25 µl reactions were used containing 400 ng each of the 3 oligonucleotide primer. PCR of DNA from wild-type animals resulted in a 450-bp fragment; from homozygous mutant animals, a 520-bp fragment; and from heterozygous animals, both a 450-bp and a 520-bp fragment.

Western blot. Mouse brains were homogenized in triple detergent buffer (100 mM Tris-HCl, pH 8.0, 150 mM NaCl, 1% Triton X-100, 0.5 mM deoxycholic acid, 1% SDS, 50 ng/ml Pefabloc, 2 U/ml aprotinin, 1 mM EGTA, 2 µg/ml pepstatin) and spun for 1 h at 100,000g at 4 °C. Protein concentration was determined using the Bradford Protein Detection kit (Biorad). Western blots were performed on the same day of protein extraction by first precipitating protein extracts (100 µg) with acetone, which was then dissolved in 1xSDS-PAGE sample buffer and run on a 4–20% premade SDS-PAGE (Biorad) for 1 h. Proteins were then transferred to Amersham nitrocellulose filter overnight at 4 °C in western-blot buffer. The filters were then probed with either GAP4 or NF1C antibodies (1 µg/ml) using a chemiluminescent kit according to manufacturer's instructions (Amersham). Both GAP4 and NF1C were previously characterized¹⁴.

Pathology. Age- and sex-matched adult mice were killed and internal organs removed for analysis. After gross examination, the tissues were fixed in 10% neutral buffered formalin. Representative tissue sections were dehydrated, embedded in paraffin, sectioned (5 µm), mounted on slides and stained with hematoxylin and eosin.

Imunohistochemistry. For the GAP4 antibody imunohistochemistry, the mice were infused through the heart with DPBS, followed by 2% paraformaldehyde in DPBS. The brains were then removed and processed for paraffin embedding. We cut 5-µm sections. Sections were boiled in sodium citrate (10 mM, pH 6) for 10 min to unmask the GAP4 antigenic site, blocked with avidin/biotin and 3% normal goat serum. Sections were then incubated with affinity-purified GAP4 antibody¹⁴ overnight at 4 °C. Primary antibodies were detected using the Vector rabbit ABC elite Peroxidase kit (Vector), enhanced by DAB enhancer, and visualized with diaminobenzidine (DAB) (Biomedica). The sections were then counterstained with aqueous hematoxylin (Xymed). The same basic procedure was used for GFAP staining using an automated immunohistochemistry stainer (Ventana Medical System 320, and rabbit anti-cow GFAP antibody (Dakopatts) at 1:1,200 dilution as a primary antibody.

Animals. For the behavioral experiments, we used group-housed males and females. The experimenters were blind to the genotype of each animal during the experiments. All the protocols used were approved by UCLA's Animal Research Committee.

Water maze. The basic protocol for the water maze experiments has been described³⁸. Our pool is circular with a 1.2-m diameter and the platform has an 11-cm diameter. The water is made opaque with non-toxic white paint and maintained at 27 °C. The movement of the mice is processed by a digital tracking device (VP118, HVS Image). During the hidden platform test, the platform was submerged (1 cm) below the water surface and maintained in the same place throughout training. The mice were given 2 trials every day (60 s ITI) for 14 d and the starting position was varied from trial to trial. In the probe trials given after 10 and 14 d of training, the platform was removed and the mice were allowed to search for it for 60 s. In the visible platform test, a distinct symmetrical cue (black and white golf ball) was fixed 5 cm above the center of the submerged platform. The animals were given 5 trials during 1 day (30 min ITI); the starting position and the platform location were pseudo-randomly varied from trial to trial.

Contextual discrimination. The contextual discrimination experiments were performed as described²¹. Chambers A and B were similar, both with grid floors and located in sound attenuating boxes in dimly lit rooms located outside the vivarium; and they were modified to have

some unique features (location, geometry, background noise, odor). Chamber C, which shared no obvious cues with chambers A and B, was located in a room inside the mouse vivarium and was brightly illuminated. This experiment consisted of three stages: pre-exposure (1 d), training (1 d) and testing (3 d). Each mouse was habituated to contexts A and B for 10 min before training started (day -1). The next day (day 0) animals were placed in chambers A and B for 3 min (the order was balanced), and after 150 s a mild foot-shock (0.75 mA for 2 s) was delivered in chamber A but not in chamber B. During the 3 consecutive testing days animals were placed in each chamber and the amount of freezing during the initial 150 s was measured. Freezing was assessed every 5 s: mice were scored as freezing if they were immobile (cessation of all bodily movement aside from respiration) for 2 s. On each of the testing days animals were shocked after 150 s in chamber A but not in chamber B. Context specificity was tested 24 h after the end of the contextual discrimination task by placing the animals in chambers A and C and measuring the amount of freezing. Long-term memory was assessed 35 d after the end of the contextual discrimination task.

Rota-rod. For the accelerating rota-rod task using a rota-rod (Ugo Basile 7650) accelerating from 4 to 40 r.p.m. in 300 s. 5 trials (35 min ITI) during the same day were given. For the constant speed rota-rod task, animals were given 4 trials (5 min) during the same day, with the rota-rod rotating at 14 r.p.m. The latency for the animals to fall from the rota-rod was measured. If the mice initiated passive rotation (that is, grabbed the rotating rod with all four paws and avoid falling) that was considered a fall.

Social transmission of food preferences. This task was performed as described^{25,26}. Mice were shaped to eat ground chow from a metal cup. First, a demonstrator mouse was removed from each cage and food deprived for 24 h. The demonstrator mouse was then allowed to eat scented food for 1 h and placed back in the cage for a period of 15 min to interact with the other mice in the cage (observers). After this, observers were food-deprived for 24 h. Finally, observer mice were tested for their preference in a 1-h test in which they had a choice between the food they smelled on the demonstrator's breath and another scented food. The amount of each food eaten (g) was measured. The demonstrated scents were pseudo-randomly assigned to each cage of mice.

Statistical analysis. A two-way ANOVA with repeated measures was used to analyze the acquisition data from the water maze and rota-rod tasks. To analyze the performance in the water maze probe trials we used a single-factor ANOVA on the percentage time in quadrant; post-hoc comparisons between quadrants were performed when there was an effect of quadrant. Planned comparisons using a paired *t*-test were used to analyze the contextual discrimination data, the proximity data in the water maze and the social transmission of food preference data.

Acknowledgments

We thank K. Thomas for the KT3NP4 neomycin cassette; R. White for support in the generation of the GAP4 antibody; D.H. Gutmann for help interpreting the immunohistochemistry; P.W. Frankland for discussions; and C.M. Spivak for inspiration and support. R.C.M. is supported by the GABBA Graduate Program (Oporto University) and the Portuguese Foundation for Science and Technology (BD 13854/97). This work was supported by a grant from the Department of Defense, U.S. Army Medical Research and Materiel Command (DAMD17-97-1-7339) to C.I.B.; grants from the NIH (R01 NS38480), the Neurofibromatosis Consortium and the Neurofibromatosis Foundation to A.J.S.; and a donation from C.M. Spivak to A.J.S.

Received 11 December 2000; accepted 26 January 2001.

- Gutmann, D.H. & Collins, F.S. von Recklinghausen neurofibromatosis. *The Metabolic and Molecular Basis of Inherited Disease* 1–19 (McGraw Hill, New York, 1994).
- Huson, S.M. & Hughes, R.A.C. *The Neurofibromatoses: A Pathogenic and Clinical Overview* (Chapman & Hall, London, 1994).
- Ozonoff, S. Cognitive impairment in neurofibromatosis type 1. *Am. J. Med. Genet.* **89**, 45–52 (1999).
- Ballester, R. et al. The NF1 locus encodes a protein functionally related to mammalian GAP and yeast IRA proteins. *Cell* **63**, 851–859 (1990).
- Martin, G.A. et al. The GAP-related domain of the neurofibromatosis type 1 gene product interacts with ras p21. *Cell* **63**, 843–849 (1990).

6. Xu, G.F. et al. The catalytic domain of the neurofibromatosis type 1 gene product stimulates ras GTPase and complements ira mutants of *S. cerevisiae*. *Cell* **63**, 835-841 (1990).
7. Brannan, C.I. et al. Targeted disruption of the neurofibromatosis type-1 gene leads to developmental abnormalities in heart and various neural crest-derived tissues. *Genes Dev.* **8**, 1019-1029 (1994).
8. Jacks, T. et al. Tumour predisposition in mice heterozygous for a targeted mutation in *Nf1*. *Nature Genet.* **7**, 353-361 (1994).
9. Silva, A.J. et al. A mouse model for learning and memory deficits associated with neurofibromatosis type 1. *Nature Genet.* **15**, 281-284 (1997).
10. Andersen, L.B. et al. A conserved alternative splice in the von Recklinghausen neurofibromatosis (NF1) gene produces two neurofibromin isoforms, both of which have GTPase-activating protein activity. *Mol. Cell. Biol.* **13**, 478-495 (1993).
11. Viskochil, D.H. Gene structure and function. in *Neurofibromatosis Type 1: From Genotype to Phenotype* (eds. Upadhyaya, M. & Cooper, D.N.) 39-56 (Bios Scientific Publishers, Oxford, 1998).
12. Zeiher, B.G. et al. A mouse model for the delta F508 allele of cystic fibrosis. *J. Clin. Invest.* **96**, 2051-2064 (1995).
13. Hogan, B., Beddington, R., Constantini, F. & Lacy, E. *Manipulating the Mouse Embryo: A Laboratory Manual* (Cold Spring Harbor Laboratory Press, New York, 1994).
14. Huynh, D.P., Nechiporuk, T. & Pulst, S.M. Differential expression and tissue distribution of type I and type II neurofibromins during mouse fetal development. *Dev. Biol.* **161**, 538-551 (1994).
15. Gutmann, D.H., Cole, J.L. & Collins, F.S. Expression of the neurofibromatosis type 1 (NF1) gene during mouse embryonic development. *Prog. Brain Res.* **105**, 327-335 (1995).
16. Nordlund, M.L., Rizvi, T.A., Brannan, C.I. & Ratner, N. Neurofibromin expression and astrogliosis in neurofibromatosis (type I) brains. *J. Neuropath. Exp. Neurol.* **54**, 588-600 (1995).
17. Rizvi, T.A. et al. Region-specific astrogliosis in brains of mice heterozygous for mutations in the neurofibromatosis type I (Nf1) tumor suppressor. *Brain Res.* **816**, 111-123 (1999).
18. Cho, Y. & Silva, A.J. Ibotenate lesions of the hippocampus impair spatial learning but not contextual fear conditioning in mice. *Behav. Brain Res.* **98**, 77-87 (1999).
19. Brandeis, R., Brandys, Y. & Yehuda, S. The use of the Morris water maze in the study of memory and learning. *Int. J. Neurosci.* **48**, 29-69 (1989).
20. Gallagher, M., Burwell, R. & Burchinal, M. Severity of spatial impairments in aging: development of a spatial index for performance in the Morris water maze. *Behav. Neurosci.* **107**, 618-626 (1993).
21. Frankland, P.W., Cestari, V., Filipkowski, R.K., McDonald, R.J. & Silva, A.J. The dorsal hippocampus is essential for context discrimination but not for contextual conditioning. *Behav. Neurosci.* **112**, 863-874 (1998).
22. Chen, C. et al. Impaired motor coordination correlates with persistent multiple climbing fiber innervation in PKC γ mutant mice. *Cell* **83**, 1233-1242 (1995).
23. Barlow, C. et al. *Atm*-deficient mice: a paradigm of ataxia telangiectasia. *Cell* **86**, 159-171 (1996).
24. Iijam, N. et al. Social interaction and sensorimotor gating abnormalities in mice lacking *Dvl1*. *Cell* **90**, 895-905 (1997).
25. Kogan, J.H. et al. Spaced training induces normal long-term memory in CREB mutant mice. *Curr. Biol.* **7**, 1-11 (1997).
26. Bunsey, M. & Eichenbaum, H. Selective damage to the hippocampal region blocks long-term retention of a natural and non-spatial stimulus-stimulus association. *Hippocampus* **5**, 546-556 (1995).
27. Upadhyaya, M. & Cooper, D.N. (eds.) *Neurofibromatosis Type 1: From Genotype to Phenotype* (Bios Scientific Publisher, Oxford, 1998).
28. Gutmann, D.H., Zhang, Y. & Hirbe, A. Developmental regulation of a neuron-specific neurofibromatosis type 1 isoform. *Ann. Neurol.* **46**, 777-782 (1999).
29. Klose, A. et al. Selective disactivation of neurofibromin GAP activity in neurofibromatosis type 1. *Hum. Mol. Genet.* **7**, 1261-1268 (1998).
30. Atkins, C.M., Selcher, J.C., Petraitis, J.J., Trzaskos, J.M. & Sweatt, J.D. The MAPK cascade is required for mammalian associative learning. *Nature Neurosci.* **1**, 602-609 (1998).
31. Brambrilla, R. et al. A role for the Ras signalling pathway in synaptic transmission and long term memory. *Nature* **390**, 281-286 (1997).
32. Largaespada, D.L., Brannan, C.I., Jenkins, N.A. & Copeland, N.G. *Nf1* deficiency causes Ras-mediated granulocyte/macrophage stimulating factor hypersensitivity and chronic myeloid leukemia. *Nature Genet.* **12**, 137-143 (1996).
33. Bollag, G. et al. Loss of *Nf1* results in activation of the Ras signalling pathway and leads to aberrant growth in hematopoietic cells. *Nature Genet.* **12**, 144-148 (1996).
34. Metheny, L.J. & Skuse, G.R. NF1 mRNA isoform expression in PC12 cells: modulation by extrinsic factors. *Exp. Cell Res.* **228**, 44-49 (1996).
35. Swiatek, P.J. & Gridley, T. Perinatal lethality and defects in hindbrain development in mice homozygous for a targeted mutation of the zinc finger gene *Krox20*. *Genes Dev.* **7**, 2071-2084 (1993).
36. Robertson, E.J. Embryo-derived stem cells. in *Teratocarcinomas and Embryonic Stem Cells: A Practical Approach* (ed. Robertson, E.J.) 71-112 (IRL, Oxford, 1987).
37. Laird, P.W. et al. Simplified mammalian DNA isolation procedure. *Nucleic Acids Res.* **19**, 4293-4294 (1991).
38. Bourtchuladze, R. et al. Deficient long-term memory in mice with a targeted mutation of the cAMP-responsive element-binding protein. *Cell* **79**, 59-68 (1994).